Titanosilicate epoxidation catalysts: a review of challenges and opportunities

Valentin Smeets,[a] Eric M. Gaigneaux,[a] Damien P. Debecker[a]*

[a] Dr. Valentin Smeets, Prof. Eric M. Gaigneaux, Prof. Damien P. Debecker
Institute of Condensed Matter and Nanosciences (IMCN)
Université catholique de Louvain (UCLouvain)
Place Louis Pasteur 1, Box L4.01.09
1348 Louvain-la-Neuve, Belgium
Email: damien.debecker@uclouvain.be
Twitter info: @deuxbeck

Dr. Valentin Smeets obtained his PhD in 2019 at UCLouvain (Belgium) in the group of Prof. Damien Debecker. His PhD thesis was dedicated to the formulation of new (hybrid) metallosilicate epoxidation catalysts. In 2020, he started a postdoctoral research project in the group of Prof. Eric Gaigneaux (UCLouvain, Belgium) in collaboration with a Swiss chemical company. His research interests include nanoparticle catalysts, mixed oxides, zeolites, mesoporous materials, sol–gel chemistry, spray-drying, hybrid catalysis, selective oxidations and hydrogenations. He is the recipient of the Advanced Porous Materials Association (Advapor) PhD Award 2020 and of the International Sol-Gel Society (ISGS) PhD Thesis Award 2019.

Dr. Eric Gaigneaux is Full Professor at Institute of Condensed Matter and Nanosciences (IMCN), Université catholique de Louvain (UCLouvain), Belgium. His main scientific interests are the preparation of heterogeneous catalysts with a control of their morphology at the atomic and nanoscopic scales, their physico-chemical characterization under operational in situ/operando conditions, and their applications in the production of biofuels, abatement of air and water pollutants, transformation of light hydrocarbons and alcohols to more valuable molecules via selective oxidation, ammoxidation, dehydration and oxidative dehydrogenation, hydrogenation of nitrogen to ammonia, and fine chemistry with a particular interest for epoxidation, Friedel-Crafts reactions and the oxidative cleavage of unsaturated fatty acids.

Damien Debecker is a Professor at UCLouvain, at the Faculty of Bio-Science Engineering. His research group – started in 2012 at the Institute of Condensed Matter and Nanosciences – focuses on the development of new heterogeneous catalysts and chemo-enzymatic catalysts, promoting more sustainable chemical processes. Targeted applications include CO_2 capture and hydrogenation, upgrading of bio-based platforms and lignocellulosic biomass to chemicals and fuels, enantioselective organic synthesis, selective oxidation, olefin metathesis, etc. Recently, he was awarded with the Young Researcher Award by the Catalysis Division of the French Chemical Society, and he is currently the holder of the Francqui Research Professor chair.

Abstract

Epoxidation reactions are tremendously important for modern chemistry, as they lead to series of highly useful bulk and fine chemicals, monomers, and intermediates for organic synthesis. Progress in epoxidation processes goes hand in hand with the advancement made in catalysis science. In this context, heterogeneous catalysts and particularly Ti-based formulations, are playing a central role and have seen tremendous developments over the past two decades, leveraging on advanced materials science. The aim of this review is to illustrate the various strategies of titanosilicates catalysts preparation that can lead to more versatile, more performant, and greener epoxidation processes. We successively cover (i) supported catalysts, obtained by the grafting of Ti species onto preformed silica supports, (ii) microporous crystalline titanosilicates (zeolites), and (iii) amorphous titanosilicate obtained by sol-gel chemistry. For each category, with an emphasis on catalyst preparation, the challenges that have to be tackled to boost catalyst performance are highlighted. From that point, we present a critical review of the different approaches that have been proposed in the primary literature to tailor the properties that govern catalysts performance (activity, selectivity, stability, ease of handling). This is done by better controlling the nature of the active surface species, adapting particles size and shape, optimizing texture, modifying surface chemistry, etc. These lines of attack encompass molecular approaches for the grafting of well-defined species, top-down and bottom-up synthesis of hierarchically porous zeolites, advanced sol-gel routes potentially performed in non-conventional media or coupled with original processing, preparation of self-standing monoliths, etc. Future research directions are discussed with emphasis on the application scope of new catalytic materials and possible approaches to increase catalyst performance.

1. Context

For more than a century, catalysis has been a pillar that supported most of the developments in industrial chemistry.[1] As sustainability is becoming a shared common objective, intensive research is currently focused on the development of cleaner, safer, and more efficient chemical processes, ideally based on renewable resources, consuming less energy and engendering less waste. [2–4] In this "technological revolution" heterogeneous catalysis has a prominent role to play, and intense research effort is being dedicated to the development of new and high-performance solid catalysts, able to operate with high atom economy, under moderate reaction conditions.[5,6]

Epoxides are key intermediates involved in the manufacture of a wide range of important commercial compounds, including pharmaceuticals, cosmetics, polymers and bulk chemicals. This reaction is a direct way to build functionality in various organic molecules including hydrocarbons; the development of greener and more sustainable epoxidation processes is a subject of considerable fundamental and industrial interest, in which catalyst preparation has a central role to play.[7] While epoxidation reactions can be catalyzed by a variety of catalysts, Ti-based formulations represent the most important class of heterogeneous epoxidation catalysts.

Ti-containing heterogeneous epoxidation catalysts consist of highly dispersed Ti(IV) species either embedded in a silica matrix (here denoted "Ti–SiO_2") or supported on a silica carrier (here denoted "Ti/SiO_2"). Industrially, the main success story of these materials is the production of propylene oxide. Since the 1970s, this commodity epoxide has been produced by the direct oxidation of propylene with organic hydroperoxides in the presence of a Ti/SiO_2 heterogeneous catalyst from Shell.[8] In the early 1980s, the discovery of the TS-1 zeolite by EniChem[9] allowed designing an alternative method for the selective epoxidation of propylene, that is utilizing H_2O_2 as the oxidant and producing water as the only side product.[10,11] It is only in 2008 that the first commercial plant using this technology was implemented by BASF and Dow in Antwerp (Belgium).[12] In 2003, Sumitomo Chemicals developed a new process for the epoxidation of propylene using cumene hydroperoxide as the oxidant.[13] This process, which targets an annual propylene oxide production higher than 1 million tons by 2022,[14] involves a mesoporous Ti–SiO_2 catalyst obtained by sol-gel chemistry, the latter being the first of its kind to have been transposed at industrial scale.[15]

There is room for improvement so as to extend the reaction scope, versatility, stability, intrinsic activity of titanosilicate epoxidation catalysts. Intense work has been undertaken in order to obtain titanosilicates that exhibit tailored physico-chemical properties and enhanced catalytic performance in epoxidation. The recent advances made specifically on hierarchical TS-1, Ti-containing zeolites, and ordered titanosilicates, were discussed in details in the reviews published in 2021 by Yu et al.,[16] in 2018 by Bellussi and Millini,[17] and in 2014 by Moliner and Corma,[18] respectively. Also, a comprehensive comparison of the catalytic performance of titanosilicate catalysts used in epoxidation can be found in the review of Přech from 2018.[19]

In this review, we focus on catalyst preparation, highlighting how the parameters that decisively determine catalytic performance can be tuned and optimized on purpose. In fact, texture and the Ti speciation largely determine the performance level. Also, particle size and morphology govern the ease of handling of the catalyst. The catalyst surface chemistry can have significant impact on the catalytic behavior as well. In the recent years, the discovery of innovative catalyst preparation techniques allowed tuning those properties and thus designing new high-performance catalysts able to work at low temperature with high selectivity and in several reactor configurations. On the one hand, zeolite-based catalysts with larger pores are developed in order to achieve higher performance in the epoxidation of bulky olefins, mostly with H_2O_2. On the other hand, highly porous and amorphous Ti/SiO_2 and $Ti–SiO_2$ bring new opportunities to catalyze epoxidation reactions in the presence of organic oxidants.

Here, we first briefly mention the different types of epoxidation catalysts (heterogeneous, homogeneous, and enzymatic), the targeted reactions, and industrial applications. Then, we focus on heterogeneous titanosilicate catalysts, highlighting the challenges that have to be tackled to design improved epoxidation catalysts. This is presented systematically for the three categories of epoxidation catalysts: (i) supported catalysts prepared by grafting, deposition or impregnation on preformed carriers, (ii) crystalline titanosilicates (zeolites) and (iii) amorphous titanosilicate obtained by sol-gel. For each category, we present a critical review of the different strategies that have recently (last two decades) been proposed in the primary literature to prepare Ti-based epoxidation catalysts with enhanced performance. We highlight the lines of attack that allow tailoring the decisive properties such as texture, particles morphology, particle size, surface chemistry, Ti dispersion, etc. We show how these parameters affect activity, stability, selectivity, and ease of handling. Finally, we reflect on future prospects of developments in the field.

2. Epoxides, epoxidation reactions, and epoxidation catalysts

2.1. Importance of epoxides in the chemical industry

Epoxides are an important class of molecules in the chemical industry. The reactivity of the epoxy group, originating from the polarity and strain of the oxirane ring, can be used to produce a large variety of products – *e.g.* diols (*via* ring-opening), lactones, carbonates – which makes epoxides ubiquitous intermediates in organic syntheses.[20] In terms of volumes, the most important epoxides are ethylene oxide (EO) and propylene oxide (PO), with a global production of about 20 million tons[21] and 8 million tons[22] per year, respectively (in 2010). Ethylene oxide is used mainly for the production of ethylene glycol, which is widely used as an antifreeze agent, or as raw material in the production of polyethylene terephthalate (PET) and polyester fibers.[23] Most of the propylene oxide produced is converted to polyols for the production of polyurethane.[24]

Other illustrative examples of epoxides are cyclohexene oxide, glycidol and epichlorohydrin (Scheme 1). Cyclohexene oxide is commonly used as a monomer in polymerization (*e.g.* aliphatic polycarbonates). It is also used in the pharmaceutical and perfume industries.[25] Glycidol possesses an additional alcohol moiety; this bi-functionality justifies its wide use as an intermediate in many sectors, from pharmaceuticals to coatings. Similarly, epichlorohydrin is an organochloride compound which finds applications as precursor in the manufacture of (epoxy) resins and polymers. The epoxidation of substituted alkenes, such as allyl alcohols, is widely used in the fine chemicals industry.[26] Similarly, many epoxides with a more complex scaffold have pharmacological or medicinal properties as well as applications in the flavor and fragrance industry. For example, fumagillin – a bisepoxide – is used as an antibiotic and geraniol (trans-3,7-dimethyl-2,6-octadien-1-ol) – a terpenic olefin – can be epoxidized to obtain fragrances, perfumes and food additives (Scheme 1).[25]

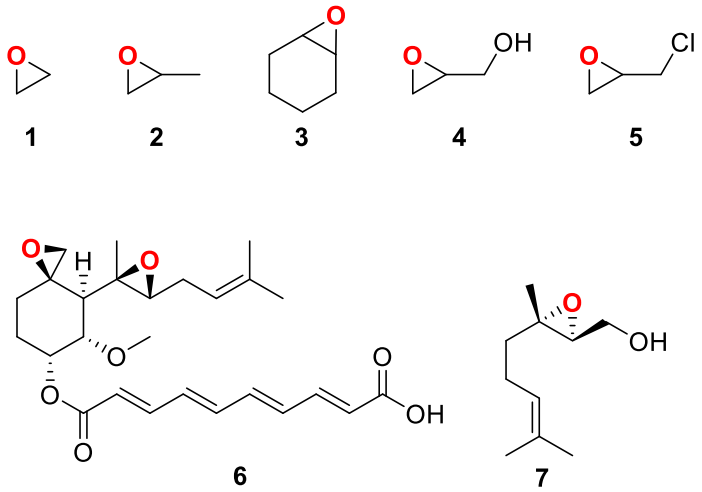

Scheme 1. Example of epoxides commonly targeted in the chemical industry: ethylene oxide (1,2-epoxyethane, **1**), propylene oxide (1,2-epoxypropane, **2**), cyclohexene oxide (epoxycyclohexane, **3**), glycidol (2,3-epoxy-1-propanol, **4**), epichlorohydrin (1-chloro-2,3-epoxypropane, **5**), fumagillin (**6**), and 2,3-epoxygeraniol (**7**).

2.2. Epoxidation reactions and common oxidants

Epoxides are produced by the addition of oxygen to a C=C double bound in a so-called epoxidation reaction. The molecule bearing the unsaturation reacts with an oxidant – typically a percarboxylic acid (*e.g.* peracetic acid, see Scheme 2), hydrogen peroxide (H_2O_2) or an organic hydroperoxide (Scheme 2) – which has been activated on an electrophilic center (*i.e.* the active site of the epoxidation catalyst). Organic hydroperoxides include for example tert-butyl hydroperoxide (TBHP), cumene hydroperoxide (CHP) and ethylbenzene hydroperoxide (EBHP). While using molecular oxygen as the terminal oxidant may appear interesting in sustainability terms, epoxidation in the presence of O_2 typically results in mediocre selectivities and is mostly restricted to the industrial production of ethylene oxide.[27–31]

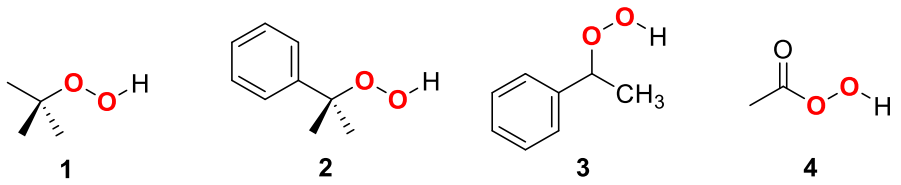

Scheme 2. Example of oxidants used in epoxidation: tert-butyl hydroperoxide (TBHP, **1**), cumene hydroperoxide (CHP, **2**), ethylbenzene hydroperoxide (EBHP, **3**) and peracetic acid (**4**).

2.3. The different types of epoxidation catalysts and processes

Epoxidation reactions are run in the presence of a catalyst, which can be either homogeneous, heterogeneous or enzymatic (Figure 1). Typically, commodity epoxides are synthesized using heterogeneous catalysts, while fine chemicals are mostly obtained *via* homogeneous catalysis. Olefin epoxidation also occurs naturally in living organisms, catalyzed by specific enzymes, which can also be exploited in artificial epoxidation reaction.

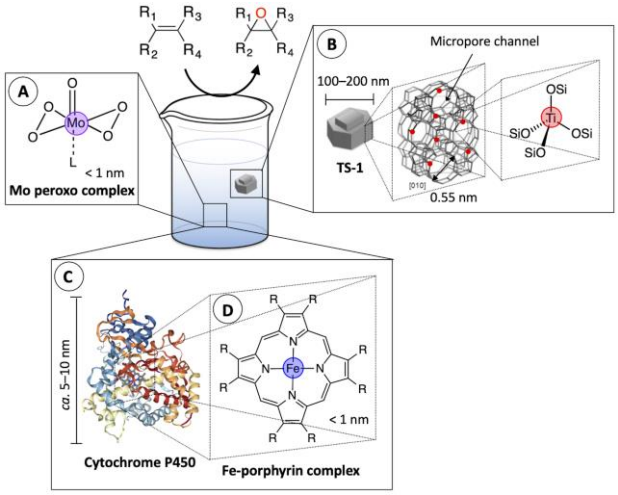

Figure 1. Schematic illustration of representative epoxidation catalysts from the three major categories: A,D = homogeneous transition metal complexes, B = heterogeneous solid catalysts, C = enzymatic (biological) catalysts.

Homogeneous catalysts – which are by definition soluble – are often optimized for one specific reaction with high selectivity and high specificity. Homogeneous catalysts are of particular interest for the liquid phase synthesis of pure enantiomers of chiral epoxides (*e.g.* Sharpless and Jacobsen-Katsuki epoxidation reactions[32–34]), with specific applications in the production of optically active pharmaceuticals and other fine chemicals. Their high turnover frequency, selectivity and specificity also come with a price: the need to recover or eliminate the catalyst from the product, which makes these systems cost-efficient only for the production of high added value chemicals. Homogeneous catalysts gather several families of compounds,[25] including i) complexes of early transition metals (Ti, Ta, V, Mo, W polyoxometalates, oxorhenium complexes) acting as Lewis acid catalysts, ii) complexes of late transition metals (Fe, Mn, Cr, Ru), acting as redox catalysts, and iii) main group elements (F, B, As, Se) forming intermediates with a structure similar to organic peroxides and percarboxylic acids.

Epoxidation of C=C bonds also naturally occurs in living organisms. Biological catalysts (*i.e.* enzymes) feature an active pocket surrounded by a precise 3D assembly of amino acids that contributes to increase the specificity/selectivity as well as to accelerate the reactions through dynamic motion of the secondary, tertiary and quaternary structures. For example, cytochrome P450 enzymes – which possess a Fe-porphyrin complex as the active center – are known to catalyze the epoxidation of olefins with molecular oxygen in order to detoxify the cells from xenobiotic chemicals,[35] as well as to produce physiologically important compounds (*e.g.* eicosanoids produced by cytochrome P450 (CYP) epoxygenases).[36–38] In addition to those naturally occurring biological functions, enzymes can be artificially engineered to generate mutants that are able to catalyze other reactions.[39,40] For example, a variant of a P450 enzyme was used to catalyze the epoxidation of non-natural substrates, such as cyclohexene and propylene.[41] Apart from P450 enzymes, peroxygenases are also capable of epoxidizing olefins in the presence of H_2O_2.[42,43]

Depending on the substrate and oxidizing agent, different types of heterogeneous epoxidation catalysts have been developed.[25,27] Many elements – including transition metals (Ti, V, Cr, Mn, Fe, Co, Nb, Mo, Ag, Ta, W, Re, Au) and metalloids (Al, Zn, Ga, Sn) – have already been reported as solid epoxidation catalysts.[44–47] These active elements are generally present as framework-substituted species in microporous or mesoporous molecular sieves (*e.g.* MFI, *BEA, and MWW zeolites, ordered mesoporous silica, aluminum-phosphate) – or as secondary cations in mixed oxides (*e.g.* V-TiO_2, Ti-SiO_2, Nb-SiO_2).[44,48–50] Alternatively, a matrix can be used as a support for well-defined metal complexes or for metals or metal oxides phases (*e.g.* TiO_2/SiO_2, Ag/Al_2O_3, Au/TiO_2, Au/SiO_2, Ga_2O_3/SiO_2, V_2O_5/TiO_2, MoO_3/Al_2O_3, V_2O_5/Al_2O_3, MoO_3/TiO_2).[46,51–55]

For example, the epoxidation of propylene is reportedly catalyzed by isolated tetrahedral Ti species supported on silica (*e.g.* Ti/SiO_2 from Shell),[8] or present in the framework of TS-1 zeolite (from EniChem).[9] These catalysts are used in liquid phase direct oxidation processes, in the presence of EBHP[56] or H_2O_2[10] respectively. Hydrogen peroxide, which is considered as a "green" oxidant since it produces water as only by-product, is generally preferred over organic hydroperoxides for the selective production of PO. Indeed, the use of H_2O_2 avoids the downstream processing of organic co-products.[24] However, the production of TS-1 can be expensive (as compared to other Ti-based catalysts) due to the use of high-purity reagents (a.o. alkali-free structure directing agent),[17,57] which means that the PO processes that utilize this catalyst could be economically more profitable by reducing the production cost of TS-1 (use of cheaper reagents, alternative synthesis routes). Alternatively, the Sumitomo process, which was developed in 2003 by Sumitomo Chemicals and accounted for about 5% of the PO production capacity in 2010,[22] involves the recycling of the alcohol co-product back to the organic hydroperoxide form (in this case CHP), positively impacting the sustainability of the process.[13] In that sense, this process is referenced as a "PO-only process".

In fact, Ti(IV)-containing silica materials are inherently active in a wide range of epoxidation reactions, on various substrates. However, several limitations have to be overcome in order to fully benefit from the intrinsic activity of these solids. This can be related to expanding substrate scope,

enhancing selectivity, increasing stability, avoiding diffusional limitations, etc. As discussed in details in Section 3, specific strategies are put in place at the stage of catalyst preparation to tackle these challenges.

3. Strategies to improve Ti-based heterogeneous epoxidation catalysts

Among all reported solid epoxidation catalysts, formulations based on Ti and silica are the most widely investigated, since they generally offer a good compromise between good catalytic performance under mild conditions and cost.[44] Also, the relative stability of the Ti–O–Si bonds usually (but not always!) prevents the leaching of the active species in liquid phase reactions.[58]

It is commonly accepted that isolated tetrahedral Ti(IV) species (*e.g.* $(\equiv Si–O)_4Ti$, $(\equiv Si–O)_3Ti(OH)$) are the most active sites in Ti-containing silica epoxidation catalysts.[59,60] These Lewis acidic Ti(IV) centers possess an oxophilic character that promotes the heterolytic activation of the oxidant to form the active intermediate.[61] In a second step, an electrophilic oxygen transfer occurs between the active intermediate and the double bond of the alkene, yielding the epoxide (Scheme 3a).

To develop good catalysts and understand their working behavior, it is important to characterize the environment of Ti-sites. To that end, DRS UV–vis spectroscopy is one of the most widely used technique to probe the coordination of the Ti centers in titanosilicates. The oxygen to tetrahedral Ti(IV) charge transfer (LMCT) band has its maximum around 200–220 nm (~ 50,000–45,000 cm^{-1}), whereas TiO_2 anatase usually appears around 310–330 nm (~ 32,000–30,000 cm^{-1}).[62] Alternatively, XPS can be used in order to quantify the proportion of Ti–O–Si and Ti–O–Ti species at the surface *via* decomposition of the $2p_{3/2}$ peak at approximately 460.0 and 458.5 eV, respectively.[63,64] Other spectroscopic techniques, such as FT-IR, Raman and XANES/EXAFS, are frequently used for the characterization of the Ti sites.[17,65–69] Finally, XRD analysis can be used to detect the presence of TiO_2 crystallites larger than the XRD detection limit based on the characteristic reflection at $2\theta = 25°$.[70]

Investigations on the nature of the active intermediate are still ongoing,[71] although monodentate $Ti(\eta^1–OOR)$ (Scheme 3b, **1**) and bidendate $Ti(\eta^2–OOR)$ (Scheme 3b, **2**) species resulting from the coordination of the hydroperoxide (ROOH) molecule on the Ti center are the most commonly accepted.[72]

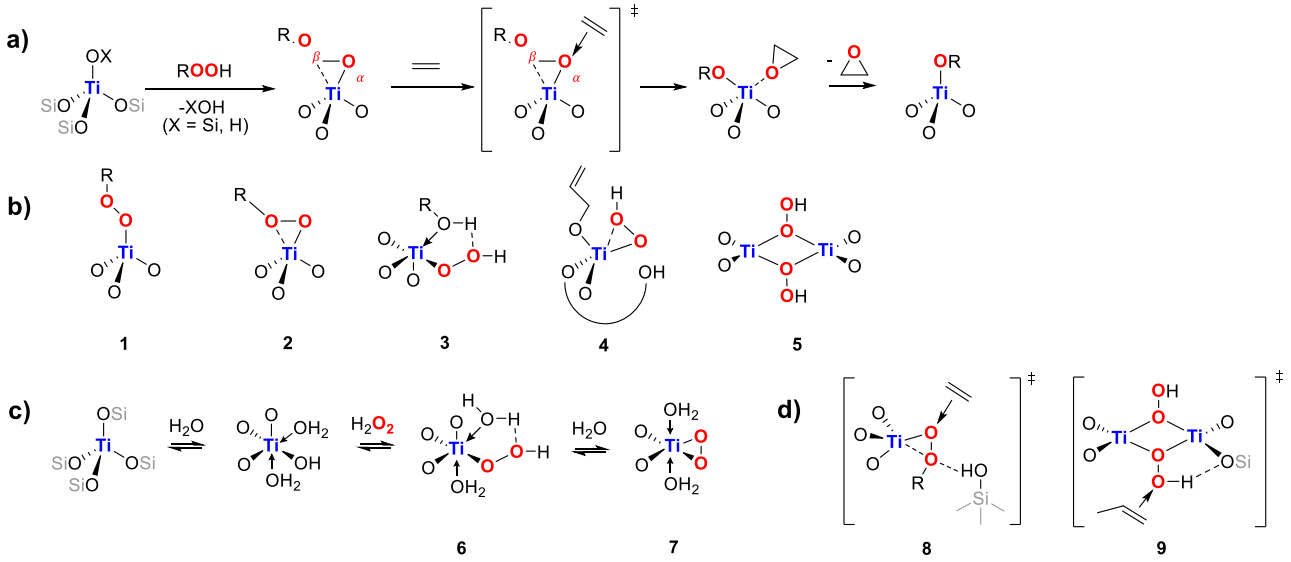

Scheme 3. a) Conventional epoxidation mechanism in the presence of Ti-based epoxidation catalysts with a Ti(η^2–OOR) (R = H, C_nH_m) hydroperoxo species (see **2** in part b) as active intermediate. The subsequent oxygen transfer from the hydroperoxo species to the alkene double bond proceeds *via* the α- oxygen, although the alkene has also been reported to attack the β- oxygen in Ti-containing polyoxometalates used as molecular models (with H_2O_2 as oxidant).[73] b) Proposed active intermediates in Ti-based catalysts: **1** = Ti(η^1–OOR), **2** = Ti(η^2–OOR), **3** = Ti(η^1–OOH)(ROH),[74] **4** = Ti(η^2–OOH)(OC_3H_5),[72] **5** = TS-1-$(OOH)_2$.[75] c) Mechanism proposed by Clerici to describe the reactivity of TS-1 in water in the presence of the H_2O_2 oxidant.[76] **6** = Ti(η^1–OOH)$(H_2O)_2$, **7** = Ti(η^2–O_2)$(H_2O)_2$. d) Transition states proposed by Katz *et al.*[77] (**8**) and Copéret *et al.*[75] (**9**) highlighting the presence of cooperative interactions between the active Ti intermediate and neighboring Si–O(H) species.

When considering the activity of TS-1 in protic alcohol solvents, it has been proposed that the solvent molecule can loosely coordinate the Ti center to stabilize the Ti(η^1–OOH) active intermediate formed in the presence of H_2O_2 (Scheme 3b, **3**).[74] Alternatively, Guillemot *et al.* suggested that the alcohol might be able to cleave a Si–O–Ti bond that releases geometric constraints around the metal center and favors the formation of an active and accessible Ti(η^2–OOH) active entity.[72] They based their hypothesis on the fact that, in the epoxidation of allyl alcohols with H_2O_2 catalyzed by a molecular model of TS-1 ($[\alpha$-B-$SbW_9O_{33}(^tBuSiO)_3Ti(O^iPr)]^{3-}$ anion), the coordination of the allyl alcohol molecule to the Ti center followed by the cleavage of a Si–O–Ti bond allow the dissociative adsorption of H_2O_2 and generate a Ti(η^2–OOH)(OC_3H_5) intermediate (Scheme 3b, **4**) that can easily transfer the oxygen from the hydroperoxo moiety to the allyl alcohol substrate (inner sphere O-transfer).

A similar mechanism has been proposed by Clerici to describe the activity of TS-1 in water with H_2O_2 as oxidant (Scheme 3c).[76] One Si–O–Ti bridge is first hydrolyzed, and the tetrahedral coordination sphere expands to an octahedral one *via* the coordination of two H_2O molecules. In the presence of H_2O_2, the ligand exchange proceeds to form the active intermediate (Scheme 3c, **6**). In TS-1, this tripodal anchoring of the titanium species is stable due to the crystallinity of the lattice, thereby making a second hydrolysis step unfavorable and thus avoiding the formation of an inert Ti(η^2–O_2)$(H_2O)_2$ peroxo species (Scheme 3c, **7**). This effect is further enhanced by the intrinsic hydrophobicity of the microporous channels as well as by the low silanol content that both limit H_2O and H_2O_2 adsorption and thus also contribute to maintain a high selectivity.[78] Indeed, studies on the stability of peroxo complexes suggested that the η^2-structure is stable only in the presence of an excess

of water.[79] In amorphous Ti-containing materials, the lack of crystalline lattice combined with the high silanol density generally do not allow to prevent the inactivation or even the leaching of the Ti species, making water a common poison for these catalysts.[80]

The usual description of the TS-1 active site and mechanism described above has been recently challenged by Copéret *et al.* who found out that the industrial TS-1 catalyst actually contains non-isolated, dinuclear Ti sites.[75] Both experimental and modelling studies suggested that bridging peroxo species formed on these dinuclear titanium sites (Scheme 3b, **5**) are responsible for the high efficiency of TS-1 in propylene epoxidation with H_2O_2, even at low temperature. These "TS-1-$(OOH)_2$" sites enable the epoxidation of propylene with H_2O_2 *via* an oxygen-transfer transition state (Scheme 3d, **9**) similar to the electrophilic epoxidation by peracids. In fact, anterior studies also suggested that high epoxidation activity does not imply that Ti oligomers should be absent from the catalyst.[81–83] Nevertheless, it is usually admitted that highly coordinated Ti species are less active and selective in epoxidation,[56] whereas pure TiO_2 typically shows no activity as it lacks free coordination sites. In the case of propylene epoxidation with H_2O_2 catalyzed by TS-1, it has been reported that amorphous TiO_2 and anatase TiO_2 present in titanium-rich TS-1 samples are responsible for the conversion of the epoxide into side products and thus for a decrease of the epoxide yield.[84] Furthermore, TiO_2 anatase phase is believed to catalyze the decomposition of H_2O_2, thereby reducing the H_2O_2 utilization efficiency (see Section 3.1).[85]

Apart from the identity of the active intermediate, structural features of the solid itself – such as the presence of neighboring defects (*i.e.* silanols) and confinement effects inside the catalyst pores[77,86–88] – have been shown to enhance the catalytic performance by stabilizing the transition state under reaction conditions (*e.g.* cooperative assemblies of hydroperoxo species bound to Ti centers with silanols,[77] see Scheme 3d, **8**). Additionally, Flaherty *et al.* have shown that the interactions within the transition state also depend on the identity and the steric bulk of the reacting species.[89]

Knowing this, different strategies can be put in place to prepare materials which feature the desired active centers. We propose to sort them in three categories: (i) supported catalysts (section 3.1), (ii) microcrystalline titanosilicates (section 3.2), and (iii) amorphous titanosilicates (section 3.3). For each category, we illustrate these types of catalysts along with their respective advantages and limitations *via* a historical overview of the developments in the field. We highlight the different guideline principles that can be followed to prepare improved catalysts.

3.1. Silica supported Ti-based catalysts

Ti-based epoxidation catalysts can be prepared by supporting Ti species on a preformed silica support. These catalysts will be denoted "Ti/SiO_2". The first Ti/SiO_2 catalyst utilized industrially for olefin epoxidation was patented by Shell in the early 1970s for the liquid phase epoxidation of propylene in the presence of EBHP with co-production of α-methylbenzyl alcohol.[8] In this process, which is known as the *styrene monomer propylene oxide* (SMPO or PO–SM) process,[56] the alcohol co-product is further dehydrated to form styrene (2.5 tons per ton of PO).[24] This process is mainly

commercialized by Lyondell and Shell,[24,90,91] and it still accounted for about 35% of the PO production capacity in 2010.[22] The Ti/SiO_2 catalyst is typically prepared by impregnating $TiCl_4$ or organic titanium compounds onto an amorphous SiO_2 support,[90,91] followed by calcination in air to form site-isolated Ti(IV) active species.[91–93] At similar reaction temperatures, this Ti/SiO_2 catalyst is as active as Mo(VI) homogeneous catalysts used in the Halcon/ARCO (now Lyondell) process developed at the same period and also dedicated to the direct oxidation of propylene in the presence of TBHP or EBHP.[94]

Since then, numerous attempts were made to design single site Ti(IV) species supported on silica-based materials (*e.g.* ordered mesoporous silicas such as SBA-15 and MCM-41, non-ordered highly porous silicas, layered crystalline silicates).[86,95–99] As compared to the one-pot synthesis of Ti–SiO_2, the grafting of Ti species onto silica supports offers the advantage to better control the location of the Ti species at the catalyst surface. For example, Ti complexes with acetylacetonate ligand immobilized on MCM-41 support exhibited higher performance for the conversion of cyclohexene with TBHP (8.8×10^{-2} s^{-1} TOF at 60°C, 96% selectivity) than Ti-MCM-41 prepared in one-pot (2.1×10^{-2} s^{-1} TOF at 60°C, 86% selectivity).[96] In supported Ti catalysts, the tunable parameters are threefold: i) the nature of the grafted Ti complex, which can be used as is or after calcination, ii) the specific surface area and the porosity of the support, which can be used to control respectively the surface density (Ti per nm^2) and the accessibility of the active sites, and iii) the surface chemistry (*e.g.* Si–OH density) and the crystallinity of the support, which respectively command the grafting of the Ti moieties and the resistance of the Ti sites against inactivation, leaching, or aggregation (see below).[100–102] The effects of these parameters are somewhat intertwined, so that it can be difficult to predict the outcome of improvement strategies. In a systematic study on delaminated SSZ-70 framework, subsequently grafted with Ti butoxide, Katz *et al.* showed that creating higher external surface area was not the key, but instead preserving the structural integrity of the crystalline zeolite was pivotal to maintain high per-Ti-site activities.[103]

Among existing strategies, the modification of the surface through a molecular precursor approach can provide effective catalysts with site-isolated Ti centers.[104,105] A good illustration is given by Ti-SBA15 which is typically prepared by post-synthesis modification of SBA-15 (specific surface area of *ca.* 500 $m^2.g^{-1}$),[106] by gas phase deposition of $TiCl_4$[97] or of titanocene dichloride,[89] or by impregnation with titanium alkoxides $Ti(OR)_4$.[107,108] These preparation methods, however, have as main disadvantage to lead to the concomitant formation of Ti oligomers with 5 to 6-coordination (Scheme 4a),[81] which usually have a lower activity compared to isolated Ti with 4-coordination.[82] Tilley and co-workers developed a thermolytic molecular precursor route[109] to graft tri(alkoxy)siloxy complexes of Ti(IV) on the SBA-15 support in order to control the dispersion of the Ti species. The formed single-site catalysts (Scheme 4b) showed excellent catalytic performance in the epoxidation of cyclohexene with CHP (TOF values up to 1.8×10^{-1} s^{-1} at 65°C), confirming again the superiority of isolated Ti species as active sites for olefin epoxidation.[110] Along this line, Ti-bridged silsesquioxanes were also used as precursors to produce silica supported Ti catalysts with isolated Ti species.[111]

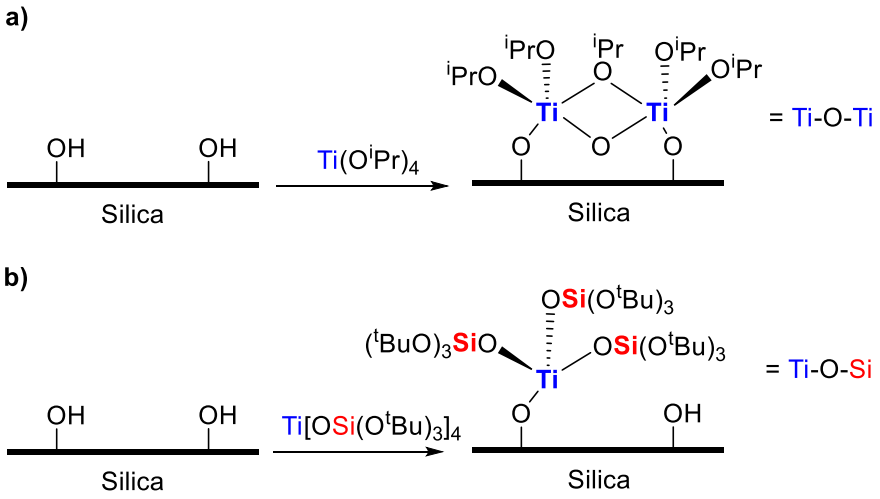

Scheme 4. Schematic representation of the Ti species in (uncalcined) Ti-SBA15 catalysts prepared by post-synthesis grafting of a) $Ti(O^iPr)_4$ and b) $Ti[OSi(O^tBu)_3]_4$. The impregnation of the support with $Ti(O^iPr)_4$ favored the side-formation of Ti dimers (5-coordination, "Ti–O–Ti"),[81] whereas the grating of $Ti[OSi(O^tBu)_3]_4$ ensured the formation of isolated Ti single sites (4-coordination, "Ti–O–Si") and resulted in higher activity.[110]

Although generally exhibiting high performance in the presence of organic hydroperoxides and in organic solvents, the activity of Ti catalysts supported on amorphous silica – which is typically hydrophilic due to its relatively high Si–OH surface density – is compromised when using aqueous solutions of H_2O_2. Indeed, water can delay the reaction by strongly coordinating the active site (*i.e.* competition with the oxidant) or hydrolyze Ti–O–Si bonds. This causes the formation of inert surface species[112] and/or the leaching of the active species.[107] Besides, it has been proposed that water can also favor Ti site aggregation.[113] Apart from its negative effect on the stability of the active sites, water can also contribute to the epoxide ring-opening toward the diol, thereby reducing the catalyst selectivity. In comparison, Ti supported onto more hydrophobic crystalline silicates typically exhibit a higher stability[102] and lead to lower diol formation. Aside from water, high local concentrations of hydrogen peroxide at Ti centers tend to favor the formation of allylic oxidation products *via* radical mechanisms, thereby negatively impacting the selectivity of the process.[101,114,115] In fact, the oxidative decomposition of H_2O_2 over Ti-hydroperoxo species is believed to result in the formation of Ti(IV)–$O^{\bullet}$ (oxyl) radicals that catalyze the decomposition of H_2O_2 and promote the hydroxylation of olefins, such as cyclohexene, at allylic positions through homolytic pathways.[76,116] In order to limit the oxidant decomposition and thus improve the H_2O_2 utilization efficiency, several solutions have been proposed, such as the use of low H_2O_2 concentrations, the slow addition of the oxidant, the reduction of the local H_2O_2 concentration around the Ti centers *via* surface hydrophobization (see below), or the use of additives that stabilize the Ti-OOH intermediate (*e.g.* phosphate monobasic anions).[116,117]

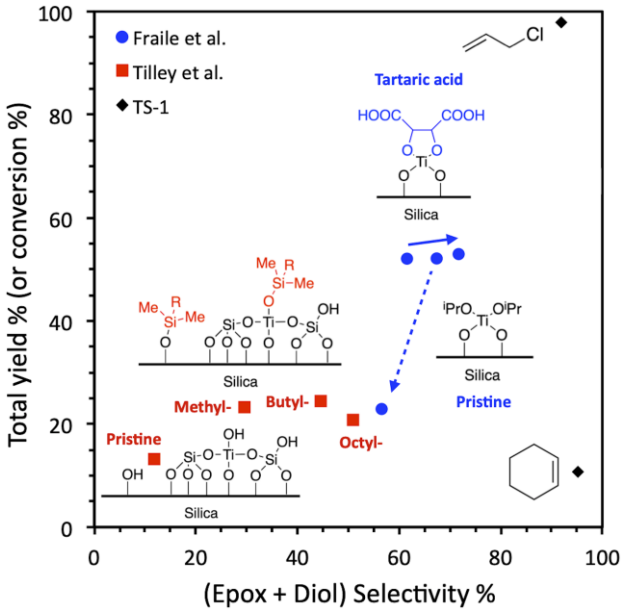

Figure 2. Impact of Ti-capping strategies used by Fraile and Don Tilley on the catalytic performance of supported Ti catalysts for the conversion of cyclohexene in the presence of aqueous H_2O_2. The "(Epox + Diol) Selectivity %" value is an indication of the proportion of epoxide formed in comparison to allylic oxidation products. The "Total Yield %" value is based on H_2O_2. The blue arrows illustrate the variations of the catalytic performance between the first and third catalytic runs for pristine and capped Ti species, as reported by Fraile *et al.*[118] Experimental conditions: T = 80°C, 1h reaction time, 50 mmol cyclohexene, 2.5 mmol H_2O_2, 200 mg catalyst (3.8 mol. % Ti), 5 ml tert-butanol (Fraile);[118] T = 65°C, 2h reaction time, 25 mmol cyclohexene, 5.5 mmol H_2O_2, 35 mg catalyst (0.13 mol. % Ti), 5 ml CH_3CN (Don Tilley).[119] Additional data for allyl chloride (T = 45°C, 0.5h reaction time, 45 mmol allyl chloride, 9 mmol H_2O_2, 310 mg catalyst [2.1 mol. % Ti], 50 ml methanol)[120] and cyclohexene (T = 70°C, 5h reaction time, 20 mmol cyclohexene, 20 mmol H_2O_2, 100 mg catalyst [1.5 mol. % Ti], 10 ml acetonitrile)[121] conversion over TS-1 are provided (see details in the text). For these catalysts, the yield is replaced by conversion values of H_2O_2 and cyclohexene, respectively.

A convincing strategy was proposed by Fraile *et al.* to improve the selectivity and stability of amorphous silica-supported Ti catalysts in the presence of H_2O_2: authors capped grafted $Ti(O^iPr)_4$ with tartaric acid (TA),[118] showing an improvement in the stability of the catalysts. While the pristine catalyst exhibited an important loss of selectivity and yield over three successive catalytic runs (see the blue dashed arrow in Figure 2), the modified complex did not show any sign of deactivation (see the blue solid arrow in Figure 2). Other capping agents (ethylene glycol, diethyl L-tartrate) were also investigated, but were shown to have a lower impact. Later on, Don Tilley *et al.* showed that the capping of Ti with hydrophobic moieties can significantly increase the selectivity of the catalysts by promoting direct epoxidation over allylic oxidation (Figure 2).[119,122] Using the pristine catalyst, the electronegativity of Ti in $(\equiv SiO)_3Ti(OH)$ favored the allylic oxidation over the direct epoxidation due to slow oxygen transfer rate from the Ti active intermediate to cyclohexene. On the contrary, the Ti sites in $(\equiv SiO)_3Ti(OMe_2R)$ were less electronegative and thus favored the production of the epoxide through the direct epoxidation mechanism.[119] This result demonstrated that the Ti electronic environment impacts the selectivity of the catalyst by acting on the oxygen transfer rate from the Ti intermediate to the olefin.[123] Another possible explanation for such gain in selectivity might be related to the local decrease of the H_2O_2 concentration around the hydrophobic Ti centers, such as also observed for Ti-silsesquioxane complexes embedded in a hydrophobic polydimethylsiloxane

(PDMS) membrane.[124] In the latter study, the H_2O_2 efficiency remained very high (≥ 97%) owing to higher [alkene]/[H_2O_2] ratios at the Ti center than in the bulk medium.

Another way out to tune the surface hydrophilic–hydrophobic properties consists in grafting hydrophobic silylation agents onto the SiO_2 support (*i.e.* capping of Si-OH groups). For example, Yamashita *et al.* proceeded to the post-functionalization of Ti-SBA-15 with triethoxyfluorosilane (TEFS).[125] Interestingly, the water adsorption capacity decreased in response to higher amounts of TEFS. By adjusting the amount of TEFS, the authors were able to increase the TON values in the epoxidation of cyclooctene with aqueous H_2O_2. Besides, although cyclooctene cannot form allylic oxidation products, the cyclooctene oxide selectivity was also very high (up to 97%) due to low diol formation. More recently, Katz and co-workers grafted an oligomeric hydrophobic capping agent (poly(methylhydrosiloxane), PMHS) onto amorphous Ti/SiO_2.[113] The authors observed a gain in stability (up to 50h on stream) in the epoxidation of 1-octene with TBHP in the presence of water as compared to pristine Ti/SiO_2 and Ti/SiO_2 functionalized with monomeric trimethylsilyl capping agent. These latter catalysts were indeed deactivated within the first 10h of time on stream. It was surmised that the capping with PMHS prevented the aggregation of Ti sites, leading to a higher resistance against water.

As an alternative to silylation strategies, Notestein *et al*. proposed in 2020 to apply an overcoating treatment with silica on Ti/SiO_2 materials in order to modify the local environment around grafted Ti species without altering the active sites or creating diffusion limitations in the solid.[126] As a result of a higher heat of adsorption of the olefin (limonene) on the SiO_2-overcoated catalyst, the latter outperformed Ti-Beta zeolite used as benchmark in terms of epoxide selectivity at 0°C. The authors argued that SiO_2 deposition could thus be used as a tool to tune the adsorption of reactants and thus increase the catalytic performance.

3.2. Crystalline titanosilicate catalysts

In the early 1980s, the discovery of titanium silicalite-1 (TS-1) by researchers from SnamProgetti (Enericerche, EniChem)[9] has allowed to overcome the deactivation and selectivity issues associated with the utilization of H_2O_2. In TS-1, single-site tetrahedral Ti are homogeneously distributed in the MFI zeolite framework by isomorphous substitution of a small proportion of the Si sites.[127] The high intrinsic stability of the TS-1 crystalline structure (see above) allowed establishing a more environmentally friendly process for the industrial production of PO, without the formation of organic co-products.[10] This *hydrogen peroxide-based propylene oxide* (HPPO) process was first developed by EniChem in the 1980s[24] and implemented twenty years later at the commercial scale by BASF and Dow in Antwerp (Belgium).[12] High activity and selectivity could be obtained under mild conditions, which favorably impacted the environmental footprint of the process (lower amount of waste and lower energy consumption). In 2010, the HPPO process accounted for approximately 5% of the PO production capacity.[22]

Despite the advantageous features of TS-1, the scope of this catalyst is mostly limited to the epoxidation of lower olefins with H_2O_2 because the diffusion of larger substrates and oxidants (such as organic hydroperoxides) within the microporous zeolite framework is constrained. Indeed, TS-1 is microporous, featuring 5.5 Å 10-membered oxygen ring channels.[60] This means that bulky molecules encounter strong intra-crystalline diffusion limitation within the micropores. In such cases, the reaction proceeds in diffusion-limited conditions, making a poor use of the catalyst (see the comparison between cyclohexene and allyl chloride conversion in Figure 2).[128] In cases where reactants cannot enter the porosity at all, the reaction is strictly restrained to the external surface. This constitutes the main limitation of such microcrystalline (zeolitic) titanosilicate catalysts. Focusing on the preparation methods, several pertinent lines of attack allow to better exploit the full potential of such formulations (Figure 3).

TS-1 is typically prepared by hydrothermal synthesis (160–170°C, 1–2 days) in an autoclave containing a clear diluted gel made of nanosized zeolite seeds. The gel is prepared under strong alkaline conditions (pH ~13 with OH^- as mineralizing agent), starting from alkoxide precursors of Si and Ti, along with tetrapropylammonium cation (TPA^+, in the form of TPAOH) as structure directing agent (SDA).[129] Alternatively, tetrabutylammonium can be used, resulting in the formation of MEL-type zeolite TS-2 that possesses similar properties.[130,131] The typical maximum Ti to (Si + Ti) molar ratio in TS-1 is of 0.025 (Si/Ti ≈ 40); higher ratios result in the concomitant formation of extra-framework Ti species.[132] The preparation and properties of microcrystalline titanosilicate epoxidation catalysts have recently been reviewed by Bellussi and Millini.[17] Rather than presenting an exhaustive review of all the existing zeolite-based epoxidation catalysts, here we aim to highlight the challenges that are inherent to the optimization of such catalysts in terms of textural and structural properties, in regard to their catalytic application. As described in the next subsections, those approaches can be divided in three categories: i) tuning the crystal size and shape, ii) increasing the pore size and/or creating additional pores, and iii) making the surface more hydrophobic.

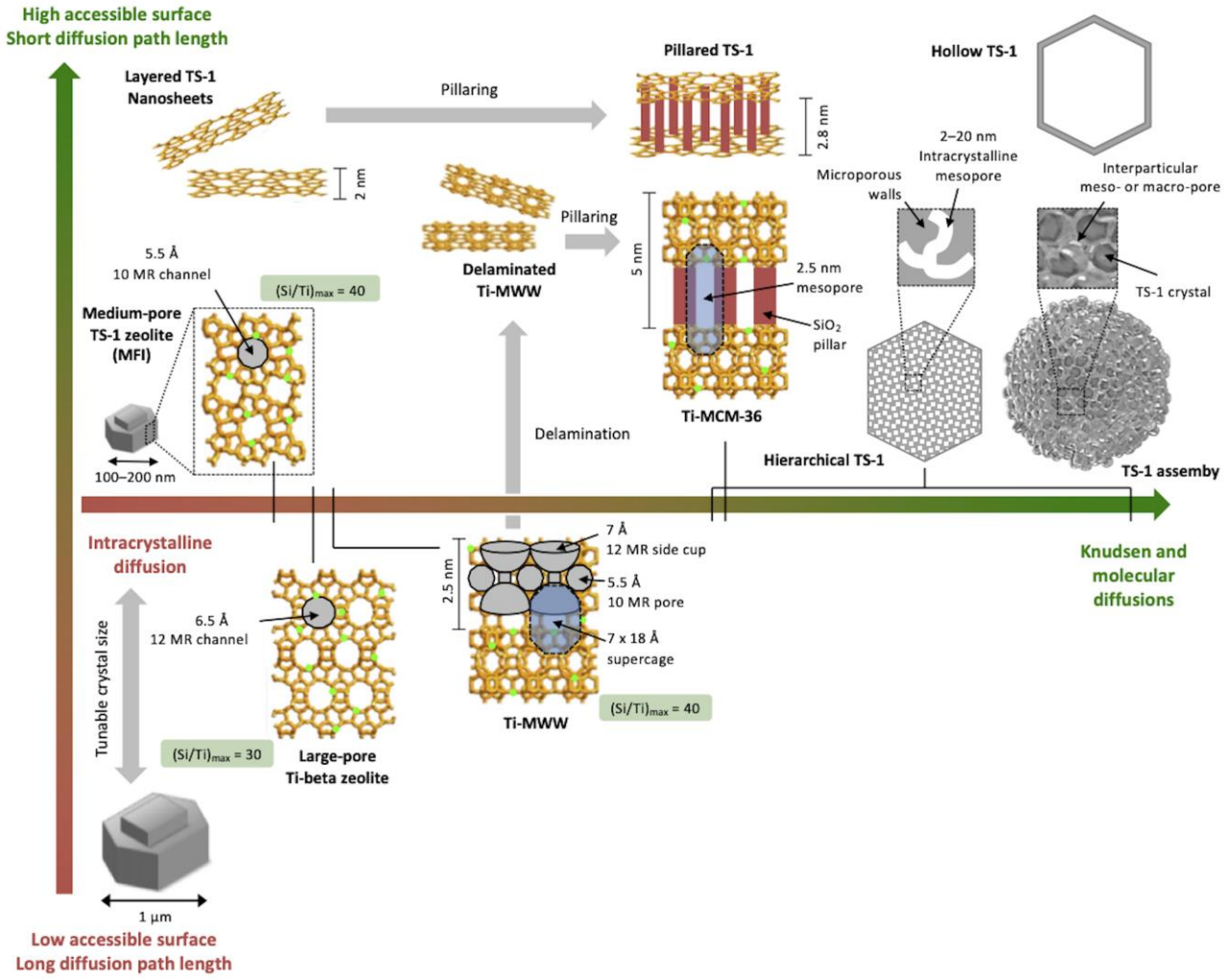

Figure 3. Illustration of the strategies used to increase the activity of crystalline titanosilicate catalysts by tuning the porosity (x-axis) and size/shape of the crystals (y-axis). The color of the arrows is an indication of the quality of the mass-transfer in the solid: red = reaction mostly limited by diffusion, green = reaction mostly limited by intrinsic activity.[128] The crystal structures have been reproduced from reference [133]. Information about porosity and structural characteristics for the most represented zeolites are also provided.[134–139] MR = Membered Ring.

3.2.1 Tuning of the zeolite crystal size and shape

For zeolitic catalysts, the elementary crystal size is a decisive parameter. If the molecules can enter into the micropores, the activity may still be diffusion-controlled and, in this case, smaller crystals having smaller the diffusion path length are more active.[140] If the microporosity is inaccessible, only the external surface area can be active, and the decrease of the crystal size increases the proportion of external surface, and boosts the activity of the catalyst.[141] Thus, intense research effort is made to develop zeolite crystals of small size, typically in the 10-200 nm range, often referred to as "zeolite nanocrystals".[142]

However, reducing the elementary particle size comes with a cost: nanocrystals are difficult to handle and recover from the reaction medium. To sort this issue, TS-1 nanocrystals can be dispersed at the surface of larger particles in order to facilitate their handling and recycling. For example, Lu *et*

al. proposed the preparation of a TS-1/modified-diatomite composite for the hydroxylation of toluene and phenol with H_2O_2 in fixed bed reactors,[143] whereas Kaliaguine *et al.* reported the coating of titanium-containing mesocellular foams (pore diameter ~30 nm) with TS-1 seeds for 1-naphtol hydroxylation.[144] Interestingly, zeolite nanocrystals can be assembled to build hierarchically porous zeolites (see section below).

Alternatively, the active site accessibility can be enhanced by preparing anisotropic zeolite crystals.[145] For example, thin zeolite nanosheets can be synthesized from two-dimensional layered precursors, *e.g.* Ti-MWW (see Figure 3). In the case of TS-1, which is not based on such lamellar precursor, the synthesis is carried out by replacing TPAOH by the $[C_{16}H_{33}–N^+(CH_3)_2–C_6H_{12}–N^+(CH_3)_2–C_6H_{13}](OH^-)_2$ surfactant as SDA, resulting in MFI nanosheets of single-unit cell thickness of 2 nm.[138] (Multi)layered MFI titanosilicates (see one illustration in Figure 4a) exhibit a very high external surface area (*ca.* 400 $m^2.g^{-1}$ *vs.* 65 $m^2.g^{-1}$ for ~500 nm isotropic TS-1 crystals). This strategy is particularly efficient, as for example Wu *et al.* demonstrated that it resulted in a 310-fold increase of the TOF in the epoxidation of cyclohexene with TBHP at 60°C.[146]

3.2.2. Tuning of the porosity

A first possibility to tune the pore size is to synthesize titanosilicate zeolites with different topologies.[18,147] Such materials range from medium-pore zeolites (4.5–6.0 Å, *e.g.* MFI TS-1, MEL TS-2) to large-pore zeolites (6.0–8.0 Å, *e.g.* *BEA Ti-Beta).[19,134,148] Ti-containing medium and large-pore zeolites are synthesized mainly by hydrothermal synthesis,[133] but they can also be obtained by post-synthesis techniques.[136] Generally speaking, the minimum Si/Ti values are in the 30–40 range.[134,135] Arguably, there is an important land of opportunities in zeolite synthesis research – with the specific aim to obtain topologies featuring larger pores – to expand the scope of epoxidation reactions. For example, van der Waal *et al.* reported a TOF value of 2.0×10^{-2} s^{-1} at 60°C for the epoxidation of cyclic norbornene with H_2O_2 on Ti-Beta zeolite, whereas TS-1 showed no activity with this substrate.[149] Similarly, when Ti-Beta was used instead of TS-1 for the epoxidation of cyclohexene with TBHP (in acetonitrile), the TOF increased by a factor of 65, in the conditions of the study.[146]

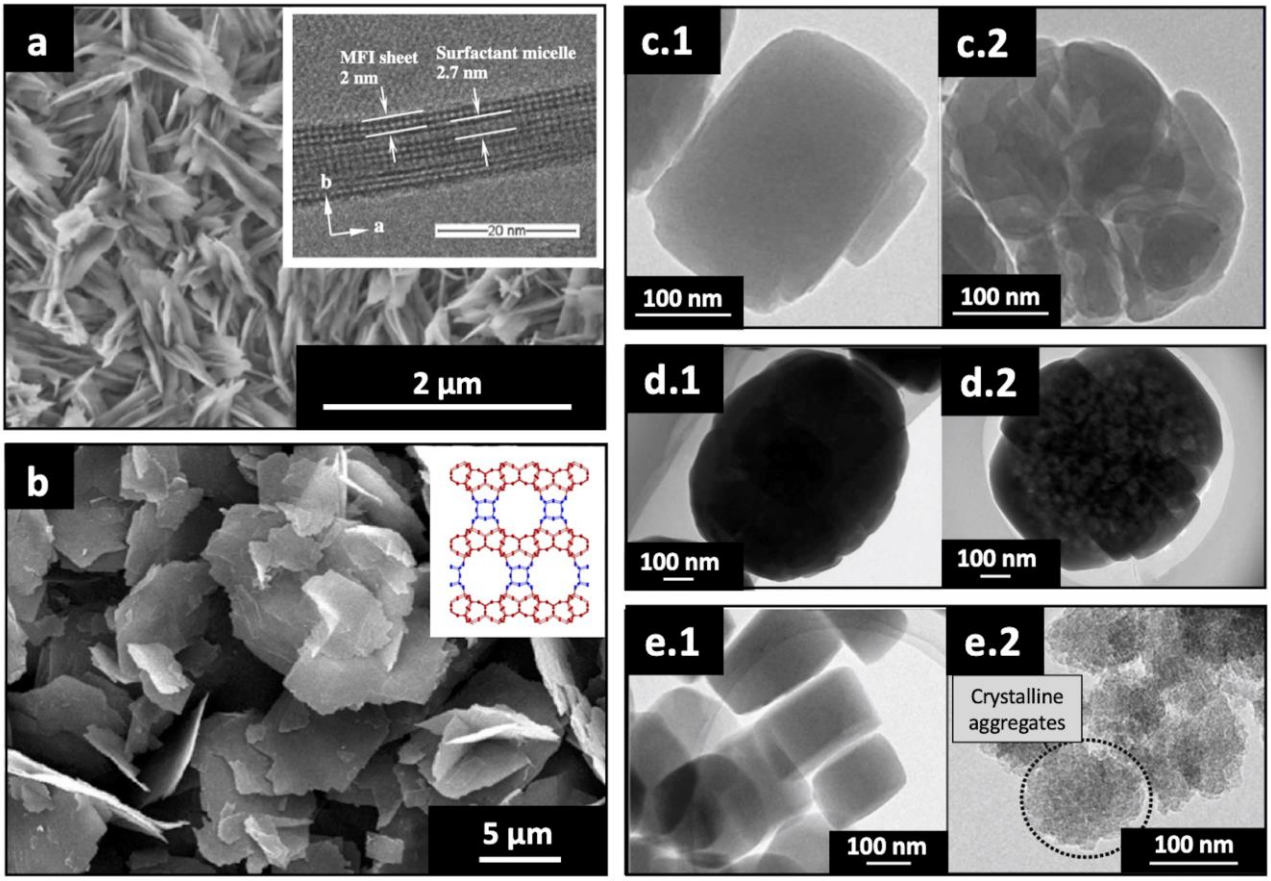

Figure 4. Microscopy images of a) multilayered MFI titanosilicate,[146] b) Ti-UTL titanosilicate (in inset is shown a schematic illustration of the zeolite structure),[150] c) conventional TS-1 (c.1) *vs.* hierarchical TS-1 obtained by post-synthetic treatment with TPAOH (top-down, c.2),[121] d) conventional TS-1 (d.1) *vs.* hierarchical TS-1 obtained by microwave-assisted post-synthetic treatment with H_2O_2 (top-down, d.2),[151] e) conventional TS-1 (e.1) *vs.* hierarchical TS-1 obtained by crystallization of functionalized zeolite seeds (bottom-up, e.2).[152] Figures adapted with permission from references [121] (Copyright 2018 American Chemical Society), [146] (Copyright 2012 Elsevier Inc.), [150] (Copyright 2015 Elsevier B.V.), [151] (Copyright 2019 Royal Society of Chemistry), and [152] (Copyright 2010 Springer Science+Business Media).

Alternatively, hierarchically porous zeolites (HPZ) can be designed so as to feature the desired crystalline structure with its associated high intrinsic activity, together with high external surface area and open entry ways that ensure faster mass transport.[128,153] For example, new large channel systems can be created in 2-dimensional lamellar zeolites to form "interlayer expanded zeolitic structures". The most represented example is Ti-MWW: this material exhibits supercages of 7 × 18 Å accessible *via* 7 Å side cup openings,[135,154] and can be delaminated or structurally rearranged to form a large variety of 3D structures.[136] For example Ti-MCM-36 is another hierarchical micro-/meso-porous zeolite made up of micropores in the crystalline layers and mesopores (2.5 nm) in the interlayer spaces.[137] Similarly, titanium can be incorporated in a UTL framework (Figure 4b) by hydrothermal synthesis to form an extra-large pore (> 8.0 Å) titanosilicate which can be further utilized as starting material for the *Assembly-Disassembly-Organization-Reassembly (ADOR)*[155] transformation to other structures.[150] The introduction of large spaces into microcrystalline titanosilicate catalysts has

been shown to have significant impact on catalyst performance, owing to facilitated diffusion.[146,156,157] In the epoxidation of cyclohexene with H_2O_2 (at 60°C in acetonitrile), Ti-MWW exhibited a TOF of 11.3 x 10^{-3} s^{-1}, whereas TS-1 reached only 2.5 10^{-3} s^{-1} (measured at low conversion, respectively 15% after 2h for Ti-MWW and 4.9% after 4h for TS-1).[157] In 2015, Přech *et al.* developed a method for the pillaring of layered TS-1, starting from TS-1 nanosheets and TEOS or a TEOS/TiBuO mixture for the synthesis of the pillars. These pillars formed ~2.8–3.0 nm spaces between individual TS-1 sheets (see Figure 3), thereby improving the accessibility to the active sites.[158] These pillared TS-1 showed higher performance than TS-1 nanosheets in the epoxidation of cyclooctene with H_2O_2.[158,159]

Another way to tune the porosity consists in the creation of a secondary intra-crystalline porosity, which can be achieved via two main approaches.[160] The first one is the post-synthetic (top-down) alkaline treatment of the zeolite crystals with *e.g.* NaOH, NH_3 or TPAOH (see Figure 4c).[151,161–163] In this case, the additional porosity is the result of partial desilication of the zeolite crystals, followed by recrystallization in the presence of the structure-directing agent.[164] As an alternative to this alkaline treatment, Park *et al.* proposed in 2018 to use H_2O_2 under microwave irradiation to generate hierarchical micro-/meso-porous TS-1 (Figure 4d), with improved catalytic activity for the oxidation of cyclohexene, cyclooctene and cyclododecene compared to TS-1.[121]

The second approach to create the additional intra-crystalline porosity is the bottom-up method, which takes place directly during the synthesis of the zeolite crystals. This procedure usually involves the use of hard or soft templates (*e.g.* surfactants, polymer beads, carbon nanotubes, carbon black).[165–169] Also, Moreno and co-workers proposed to prepare hierarchical TS-1 (see Figure 4e) *via* the functionalization of zeolite seeds (pre-formed in a liquid gel or in an amorphous Ti–SiO_2 xerogel) with organosilanes prior to the crystallization step.[152,170] In these hierarchical zeolites, the presence of the secondary mesoporosity was proved to be beneficial to the catalytic activity. In the conditions of this study, the TOF value for the epoxidation of cyclohexene with TBHP at 100°C increased from 1.5 × 10^{-2} s^{-1} for TS-1 to 6.5 × 10^{-2} s^{-1} for the micro-/meso-porous zeolite.[152] Moreover, hierarchical zeolites can be obtained by crystallization under supersaturated conditions. The so-called *steam assisted crystallization* (SAC) method has become a popular procedure to prepare hierarchically porous zeolites.[171,172] In this method, an amorphous Ti–SiO_2 mixed oxide is prepared in the form of a dry gel and treated under hydrothermal conditions in the presence of a structure-directing agent and of steam. Upon steaming, the crystallization of the zeolite has been suggested to proceed via an oriented attachment route, which consists in the aggregation and alignment of tiny crystallites that form bigger crystals.[173] The porosity is typically controlled in the mesoporous range by the addition of templates – *e.g.* organosilanes – that prevent the fusion of the crystallites,[174] or by leveraging on the grinding and drying steps of the gel prior to autoclaving.[166] Using this method, He *et al.* obtained micro-/meso-porous TS-1 crystals with 20 nm mesopores and exhibiting *ca.* 10-fold higher conversion than benchmark TS-1 when tested for the hydroxylation of phenol with TBHP (70°C, 4h).[174]

When targeting the creation of secondary macropores, the post-synthetic approach – *e.g.* controlled dissolution of the zeolite framework with etching agents[175,176] – is often preferred. An elegant example is the case of hollow TS-1 crystals.[177,178] However, macropores have also been obtained *via* bottom-up strategies.[179,180] Here, amorphous Ti–SiO_2 nanoparticles are used both as Ti and Si precursors and as hard templates during the crystallization process. Upon hydrothermal treatment in a steam atmosphere (SAC, see above), the Ti–SiO_2 nanoparticles dissolve and provide the Si and Ti precursors for the crystallization of the MFI framework that progressively forms around the precursor nanoparticles, resulting in the creation of intracrystalline macropores (Figure 5).[181] Owing to the improved mass transfer properties and the conservation of high external surface-to-volume ratios, this strategy was effective to maintain high catalytic activity while increasing the crystal size. Importantly, such large hierarchically porous particles are easier to handle and recover, which would facilitate their application at the industrial level, as compared to zeolite nanocrystals.

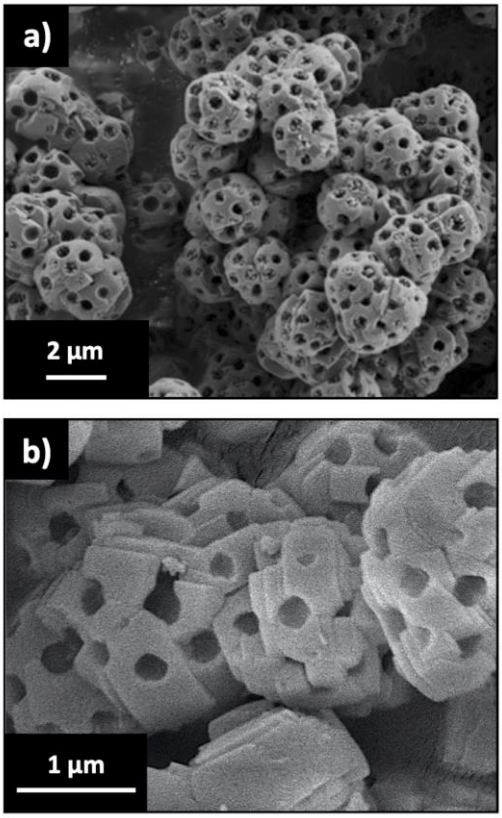

Figure 5. SEM micrographs of hierarchically porous (micro-macro) TS-1 epoxidation catalysts obtained by steam-assisted crystallization from a) Schwieger *et al.*[179] and b) Debecker *et al.*[180] Part (a) adapted with permission from reference [179]. Copyright 2019 Wiley-VCH Verlag GmbH & Co. KGaA.

Alternatively, the macroporosity originates from inter-crystalline spaces between individual TS-1 building blocks assembled together in larger hierarchical assemblies. These can be obtained by crystallization of a macroscopically structured dry gel containing the zeolite nanocrystals.[182–184] For example, the controlled drying of TS-1 colloidal suspension has been used by Mintova *et al.* for the synthesis of hierarchical TS-1 with enhanced adsorption properties.[185] Similarly, aerosol processes

can be used to assemble zeolite nanocrystals and form larger particles of HPZ.[186,187] We consider these processes as highly promising, because they can be operated in a continuous mode, and are considered to be easily scalable and to produce relatively low amounts of waste.[188] Importantly, the aggregation allows benefiting from the high surface-to-volume ratio of the zeolite nanocrystals, while also manipulating particles in the micrometer range. Thus, Schwieger *et al.*[189] and Xiong *et al.*[190] used such spray-drying method to assemble silicalite-1 and TS-1 nanocrystals into microspheres displaying a hierarchical porosity (Figure 6). The hierarchical titanosilicate synthesized by Xiong *et al.* exhibited a two-fold increase in cyclohexene conversion (60°C, 6h) in the presence of H_2O_2 as compared to regular TS-1, as a result of the exposure of more TS-1 outer surface in the hierarchical assembly. Moving further, such a spray drying approach was recently exploited to prepare large hollow zeolite microspheres featuring micro-, meso- and macropores.[191] These particles were shown to both (i) efficiently catalyze the epoxidation of allyl alcohol and (ii) be able to host aggregates of an enzyme (glucose oxidase) which serve for the in situ production of H_2O_2. This concept provides avenues for the future development of chemo-enzymatic processes with zeolite catalysts and enzymes, not only in the field of epoxidation.

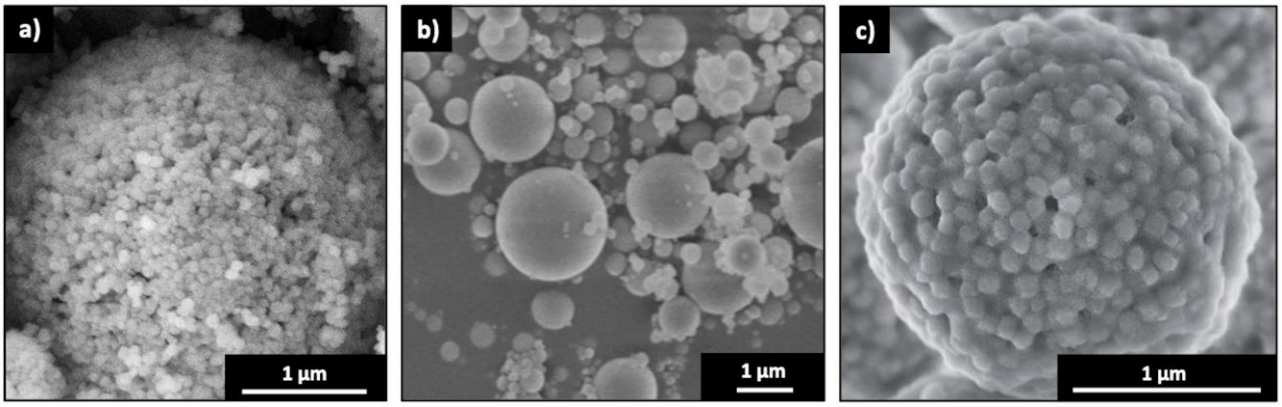

Figure 6. SEM images of hierarchically porous zeolite microspheres obtained by the spray-drying of nano-crystals of silicalite-1 (a)[189] and TS-1 (b–c).[190,191] Part (a) adapted with permission from reference [189]. Copyright 2016 Elsevier Inc. Part (b) adapted with permission from reference [190]. Copyright 2015 Springer Science+Business Media.

3.2.3 Enhancing surface hydrophobicity

Modifying the polarity of the surface of heterogeneous catalysts is known as a relevant strategy to boost the performance because it directly affects the rates of reactants adsorption and of products desorption.[192–196] Microporous crystalline titanosilicate catalysts are intrinsically less hydrophilic as compared to their amorphous mixed oxide counterparts, owing to textural effects and to the low number of defects. In the case of olefin epoxidation with Ti-based zeolites, however, increasing surface hydrophobicity can help further boosting conversion and selectivity, mostly because a more hydrophobic surface favors the adsorption of the olefin and the desorption of the epoxide, thereby decreasing the residence time of the product on the catalyst surface and thus the probability of ring-opening to the diol.

This was demonstrated with Ti-beta zeolites grown in the presence of fluoride ions, which – as compared to the regular Ti-beta catalyst – showed higher hydrophobicity and higher rates in the epoxidation of methyl oleate with H_2O_2.[197] Using a post-synthetic fluoride treatment on nanosheet TS-1, Ryoo and co-workers[138] managed to decrease the concentration of silanols, making the surface less hydrophilic. This had a marked positive impact in the epoxidation of bulky olefins (*e.g.* cyclooctene). A similar strategy was applied on the MWW-type titanosilicate, with again a strong positive effect on catalytic performance in the epoxidation of 1-hexene in acetonitrile, with H_2O_2 as the oxidant.[198] However, apart from a clear effect of hydrophobicity, authors argued that the treatment also provoked an increase in Lewis acid site strength, which also participates in the activity boost, so that it is delicate to draw definitive conclusions in this case. Interestingly, the use of polymer beads to add a secondary porosity in the zeolite (as discussed above) has been claimed to also somehow result in a modification of the catalyst hydrophilicity: Song *et al.*[169] claimed that the enhancement in propene epoxidation activity observed with TS-1 catalysts templated with polystyrene or polymethylmethacrylate beads was related to a higher hydrophobicity, as compared to untemplated TS-1. Moving further, Chen *et al.*[199] utilized a one-step hydrothermal route to synthesize a TS-1-based catalyst in the presence of resole resin precursors to bring a more hydrophobic character in the catalyst. Upon the application of a specific carbonization and thermal treatment in N_2, TPAOH is effectively removed, a typical MFI structure is obtained, but residual aromatic species are also maintained in the materials. The higher hydrophobicity of the latter was demonstrated by contact angle measurements, and the new catalysts featured enhanced selectivity for propene epoxidation with H_2O_2.

Counterintuitively, Flaherty *et al.*[200] have shown in 2019 that hydrophilic Ti substituted zeolites *BEA, possessing a high density of silanol nests $(SiOH)_4$, were more active than their hydrophobic (*i.e.* defect-free) counterparts when catalyzing the epoxidation of 1-octene with H_2O_2 in the presence of water. In particular, small clusters made of adsorbed water molecules were confined inside the pores in the vicinity of the $(SiOH)_4$ groups. These confined water clusters may rearrange upon the adsorption of the reactants and the formation of the transition state, resulting in a change of excess free energy and ultimately an increase of the reaction rate up to 100 times as compared to the defect-free zeolite.

Thus, the synthetic strategies that allow tuning the hydrophilicity or hydrophobicity of microcrystalline Ti-based epoxidation catalysts are numerous and this undeniably constitute an important line of attack for catalyst development.

3.3. Amorphous Ti-SiO_2 catalysts

The quest for large-pore Ti–SiO_2 catalysts started in the early 1990s and was motivated by the possibility to overcome the limitations encountered with zeolites in terms of active site accessibility. As compared to zeolite catalysts (see section 3.2), amorphous titanosilicates show more flexibility in terms of texture and composition. This offers a series of advantages for the expansion of the reaction

scope of Ti–SiO_2 catalysts towards the conversion of bulky substrates (*e.g.* cyclic olefins or olefins present in plant oils[201,202]). The first examples of amorphous Ti–SiO_2 were described in 1994 by Corma *et al.*[100,203] and Pinnavaia *et al.*,[204] who respectively reported the one-pot synthesis of Ti-MCM-41 and Ti-HMS molecular sieves. These ordered mesoporous materials exhibit well-ordered and uniform mesopores (2.0–3.5 nm for Ti-MCM-41[100] and 4.3 nm for Ti-HMS[106]) surrounded by amorphous walls.

The challenge related to the preparation of efficient amorphous Ti-SiO_2 epoxidation catalysts are related to (i) controlling the Ti speciation, (ii) maintaining good textural properties and (iii) facing the inactivation of Ti active sites and/or leaching in the presence of water. To tackle those challenges, the catalyst preparation has to be mastered. Amorphous Ti–SiO_2 are typically obtained by bottom-up sol-gel routes,[205–207] which represent a powerful toolbox for the one-pot bottom-up preparation of amorphous metallosilicates used as solid catalysts.[207–209] Starting from molecular precursors, the methods rely on a succession of hydrolysis and condensation steps taking place in aqueous solution. During the hydrolysis step, inorganic molecular precursors (*e.g.* alkoxides) are put in solution and allowed to hydrolyze to form the reactive gel precursors. During the condensation step, these precursors react to form oligomers in which the elements are bound *via* oxo-bridges (*e.g.* siloxane bonds, Si–O–Si, in silica). Upon oligomerization, the solution first turns into a sol. Then, upon reticulation, a wet gel is formed. This gel often undergoes a subsequent step of ageing before it is dried and finally calcined to remove the organics. By mixing precursors of Si and Ti, titanosilicate materials can be obtained. Furthermore, sacrificial templates can be introduced in the precursor solution so as to introduce porosity in the gel (see section 3.3.2). These templates are typically removed by calcination or washing.

In this section, we describe recent developments in the field of sol-gel routes to amorphous Ti–SiO_2, keeping the focus on the different strategies than can be implemented to enhance the performance of such catalysts in epoxidation reactions. In particular, we highlight three main strategies to boost the performance of Ti–SiO_2 epoxidation catalysts. Through selected examples, we show that tweaking the sol-gel chemistry process allows enhancing catalyst performance. In fact, by optimizing the preparation procedure and depending on the applied reaction conditions, amorphous Ti–SiO_2 can be up to 10^3 times more active than medium-pore zeolites for the conversion of bulky molecules (*e.g.* cyclic olefins, see Figure 7).

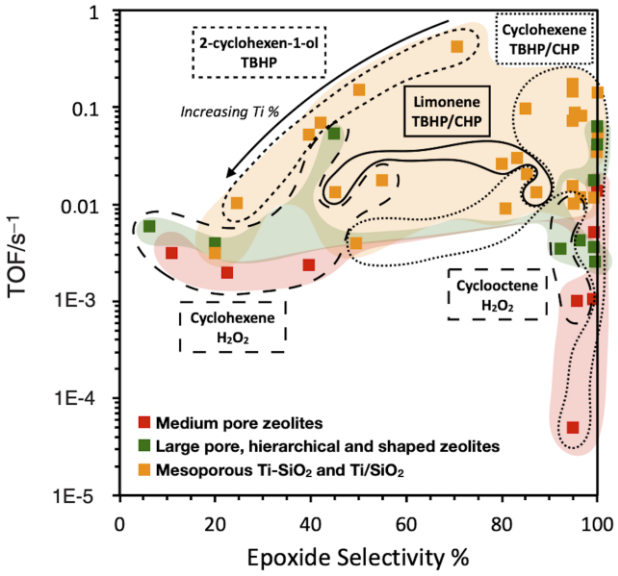

Figure 7. Comparison of TOF values for the conversion of cyclic olefins over Ti-containing catalysts: medium pore zeolites, large pore, hierarchical and shaped zeolites, and mesoporous Ti-SiO_2 and Ti/SiO_2.[25,50,82,96,110,130,146,152,183,190,210–216] These catalysts are mostly used with organic hydroperoxides (TBHP, CHP). For more examples, see the review of Přech.[19] Only few (mostly unsuccessful) attempts were made using aqueous H_2O_2 with amorphous titanosilicates and Ti-supported catalysts. We draw the attention of the reader on the fact that the present figure should be seen as a guide to the eye, since the TOF and selectivity values gathered here have been obtained under various reaction conditions (temperature, olefin and oxidant concentrations, solvent).

3.3.1. Improving the Ti dispersion

Considering the working principles of sol-gel chemistry, amorphous Ti–SiO_2 can incorporate a higher amount of Ti compared to zeolites.[217,218] According to Evans, the solubility of Ti in amorphous silica can be decomposed into three domains (Figure 8).[219] Mobilio *et al.* reported that from 0 to 8.9 mol.%, Ti can be statistically dissolved in the silica framework without forming a separate phase (“stable” region); between 8.9 and 12.5 mol.%, Ti oligomerization begins to occur (“metastable” region); and above 12.5 mol.%, Ti cannot be fully dissolved in the silica matrix, leading to the formation of TiO_2 domains (“unstable” region).[220] Ti species in these three regions exhibit very different catalytic behaviors.

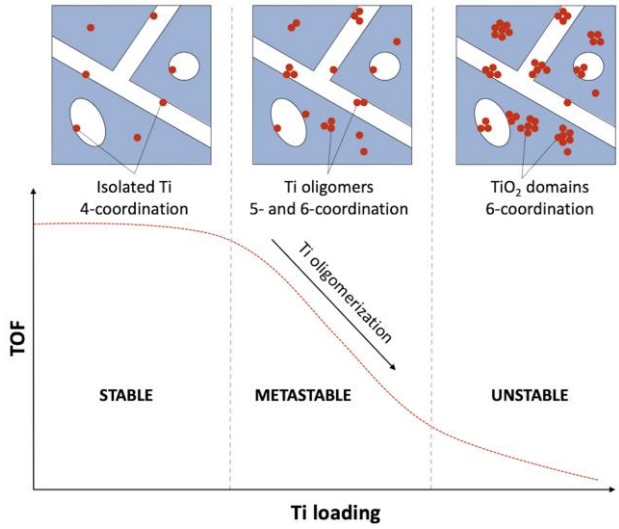

Figure 8. Typical structure-activity relationship in amorphous Ti–SiO_2 catalysts. The upper side of the figure is a schematic representation of the three domains of solubility for Ti in silica.

Indeed, amorphous titanosilicate catalysts show a strong structure-activity relationship: poor dispersion is related to a larger proportion of highly coordinated Ti species and thus results in a lower activity per active site (TOF).[82,215,221,222] This issue gets more pronounced when increasing the Ti loading (Figure 8). The inherent limitations of classic sol-gel chemistry can be rationally explained by the molecular structure and the relative reactivity of Ti and Si precursors. On the first hand, Ti precursors are prompt to spontaneous oligomerization due to the tendency of tetrahedral Ti to expand its coordination sphere.[223] On the second hand, in (hydrolytic) sol-gel chemistry, Ti precursors generally condense much faster than Si precursors, thereby kinetically favoring the formation of oligomers of Ti oxide trapped in a silica matrix at the expense of Ti inserted in tetrahedral coordination in silica. Therefore, the main challenge is to control the quality of the Ti dispersion in the silica framework.

Different strategies have been developed in order to level off the reactivity of the Ti and Si precursors, such as the pre-hydrolysis of the precursors in acidic or alkaline conditions – in which the condensation rates are low[224] – and the utilization of reactivity modifiers.[225,226] In 2014, Rankin *et al.* reported the one-pot synthesis of amorphous Ti–SiO_2 thin films in the presence of a sugar-based surfactant (η-dodecyl β-D-maltoside) used as complexing agent for titanium propoxide precursor.[227] This pre-complexation step – during which preferential interactions were generated between the Ti alkoxide and the maltose head groups – was shown to promote a homogeneous distribution of Ti with high dispersion (UV-vis) by preventing the fast condensation of the Ti precursor during the gel formation.

Alternatively, the aerosol-assisted sol-gel process (Figure 9) exploits the atomization of the precursors solutions and the fast drying of the so-formed droplets to kinetically quench the formation of the metallosilicate, thereby providing a facile way of enhancing the metal dispersion and

homogeneity.[187] Using this method, it is possible to integrate i) reactive sol-gel chemistry starting from molecular precursors and leading to the desired metallosilicate, (ii) texture templating via the utilization of sacrificial pore generating agents, and (iii) microparticles formation whose size and shape can be tuned by playing on the process operation conditions. The aerosol-assisted sol-gel method was used to prepare hierarchically porous Ti–SiO_2 microparticles successfully exploited as epoxidation catalysts.[228] To ensure a good Ti dispersion, the syntheses were carried out in alkaline conditions in the presence of TEOS and $Ti(BuO)_4$ as Si and Ti precursors, respectively. Owing to the fast-drying conditions, the gel composition was quenched, ensuring a homogeneous distribution of Ti (ICP-AES, XPS), mostly incorporated as tetrahedrally coordinated sites (XPS, UV-vis), conferring high epoxidation activity. As discussed in the next section, these catalysts also benefited from tailored textural properties that decisively impacted the performance.

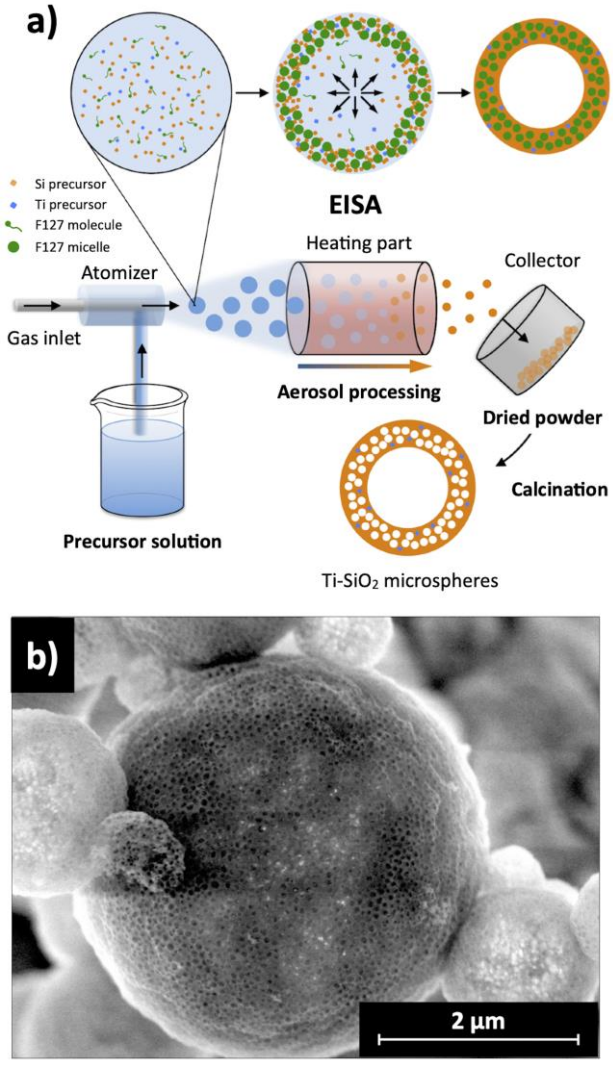

Figure 9. Preparation of mesostructured Ti–SiO_2 by the aerosol process. a) Schematic illustration of the aerosol set-up along with the evaporation-induced self-assembly (EISA) mechanism, b) SEM image of a hierarchical Ti–SiO_2 catalyst made by aerosol with polystyrene polymer beads as additional hard macroporous templates.[228]

In another approach, the classic hydrolysis-condensation reactions can be replaced by non-hydrolytic solvolysis and condensation reactions. In such non-hydrolytic sol-gel (NHSG) route, water

is replaced by organic molecules (alkoxide, alcohol, ether, etc.) as oxygen-donors.[229–233] These conditions offer a better control over the condensation kinetics of the precursors (halide, alkoxide, acetylacetonate, etc.) as they involve higher activation energies.[234] In 2015, Pinkas *et al.* used titanium(IV) diethylamide and silicon tetraacetate as precursors to synthesize amorphous Ti–SiO_2 via the acetamide elimination route.[235] A high Ti dispersion was maintained up to 11.5 mol.% Ti (UV-vis), thus close to the solubility limit of Ti in silica (see above). The authors reported that the use of Pluronic P123 as sacrificial pore template (see section 3.3.2) contributes to the stabilization of the tetrahedral Ti species upon the calcination of the gel – *i.e.* it prevents the oligomerization between neighboring Ti species by weakly coordinating the metal. The catalysts were tested in cyclohexene epoxidation with cumyl hydroperoxide in toluene. Calcination was shown to be a key step to increase the activity of amorphous Ti–SiO_2 prepared by NHSG.[216,236] Indeed, the heating of the gel – which is associated with an increase of the degree of Si–O–Ti cross-linking[236] – was shown to prevent Ti leaching during the catalytic reaction[235] as well as to increase the SSA due to the elimination of unreacted organic moieties on Si and Ti.[236]

3.3.2. Improving the texture

Extending the applicability of amorphous Ti–SiO_2 catalysts to a wider range of substrates often requires the development of formulations that feature a high specific surface area and/or large pores. For porous catalysts, when the process is diffusion-limited, particle size reduction means a higher proportion of external surface and can lead to higher activity. It has been shown that the addition of polydiallyldimethyl ammonium chloride – a cationic polymer – during the one-pot synthesis of Ti-MCM-41 allows reducing the particle size from the micrometer scale to 40–75 nm, which resulted in improved cyclohexene epoxidation in the presence of H_2O_2.[237] Also, the diffusivity can be improved by 2 or 3 orders of magnitude when switching from micropores to meso- and macropores.[128] The most significant progresses in this direction were obtained thanks to the development of sol-gel routes leading to large-pore amorphous Ti–SiO_2.

Nevertheless, creating a more open porosity is not straightforward. Under aqueous sol-gel synthesis conditions, the high surface tension of water often leads to pore shrinkage and collapse when the gel is being dried towards the "xerogel" state.[238,239] To solve this issue, one can rely on three main types of strategies: (i) utilization of sacrificial pore-generating templates, (ii) application of peculiar processing techniques for synthesis and drying, and (ii) exploitation of non-hydrolytic synthesis conditions.

3.3.2.1. Tuning catalyst texture with sacrificial templates

Templating strategies have long been developed to form materials which, upon calcination or washing, exhibit the desired porosity. For example, the mesopores of Ti-MCM-41 are generated by the use of hexadecyltrimethylammonium bromide (CTAB), a surfactant which forms micelles around which the polycondensation of the titanosilicate takes place, and which is subsequently removed to

create a calibrated porosity. Similarly, Ti-HMS is obtained by the use of dodecylamine (DDA). Pluronic surfactants are also widely used as soft template in the preparation of mesoporous silicates[240] and titanosilicates (*e.g.* Ti-MCM-41, see above).[241,242] For example, in 2012, Vinu *et al.* proposed the synthesis of mesoporous Ti–SiO_2 in acidic conditions using F127 as template.[243] These catalysts possessed high specific surface areas in the 770–940 $m^2.g^{-1}$ range associated with the formation of 5–7 nm mesopores. These materials exhibited high performance for the epoxidation of cyclohexene with TBHP (up to 86% conversion after 6h at 60°C, with 72% selectivity towards cyclohexene oxide). In fact, a plethora of surfactant-assisted sol-gel synthesis of highly porous catalysts can be found in the literature.[244] Rather than presenting an exhaustive review of all these systems, we highlight recent sol-gel routes that led to significant advance in epoxidation processes, thanks to the utilization of original sacrificial template.

In 2017, Balkus and co-workers[214] reported the synthesis of Ti-containing wrinkled mesoporous silica materials coined "Ti-WMS" using microemulsions (water-1-butanol-cyclohexane system) as template.[245] These catalysts featured 3 nm mesopores and were used as epoxidation catalysts for cyclohexene with TBHP, outperforming Ti-MCM-41 by ~1 order of magnitude in terms of TOF (at 60°C in acetonitrile). The enhancement of the activity was explained by a 360° diffusion through the radial structure of the material, which differs from the mono-directional diffusion that is imposed in the hexagonal structure of MCM-41 (Figure 10).[214]

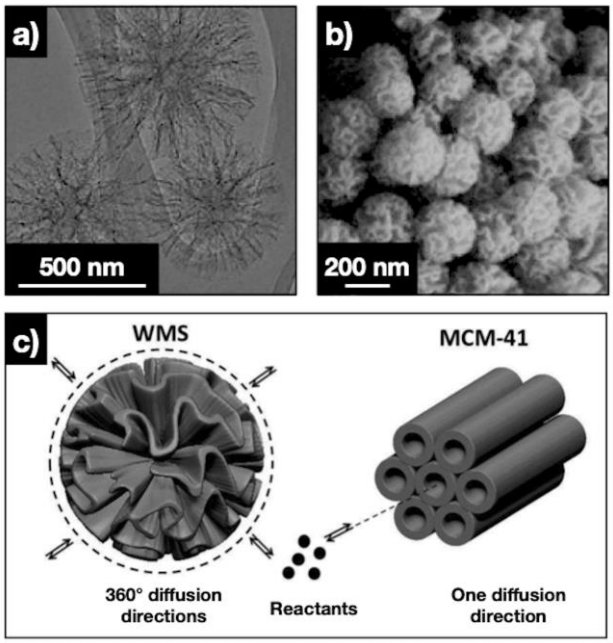

Figure 10. a) TEM and b) SEM images of Ti-WMS prepared with a Si/Ti ratio of 40, c) Schematic illustrations of the WMS and MCM-41 type catalysts. The former was reported to be one order of magnitude more active than the latter in the epoxidation of cyclohexene with TBHP. Reproduced with permission from reference [214]. Copyright 2017 Elsevier Inc.

Oki *et al.* used alkyl amines as templates in the synthesis of mesoporous Ti–SiO_2 in acidic media, resulting in the formation of mesopores in the 1.8–11 nm range.[246] These catalysts exhibited higher

cyclohexene conversion compared to a control Ti–SiO_2 catalyst prepared without template. The level of activity could be correlated with the gain in SSA resulting from the creation of mesopores. In another successful approach, Bruce *et al.* proposed polypropyleneimine dendrimers as pore-directing agents for amorphous Ti–SiO_2 (pore size of 1.2–1.3 nm with S_{BET} in the 500–640 $m^2.g^{-1}$ range).[247] These catalysts were 100% selective towards the epoxide in the oxidation of cyclohexene with TBHP. Besides, the authors observed a correlation between the reaction rates and the pore size, itself being dependent upon the size of the dendrimer used to create it.

Specific templating strategies can also be used to obtain macroscopic and self-standing materials instead of fine powders. In 2014, Hüsing *et al.* reported the synthesis of hierarchically porous Ti–SiO_2 monoliths under aqueous conditions (Figure 11a).[248] The synthesis was based on the sol-gel processing of a single source precursor made of glycol-modified organofunctional silanes tethered to a titanium center. Under acidic conditions, the condensation of the water-soluble glycolated silanes induced phase separation at a macroscopic length scale. The use of block-copolymer P123 surfactant further contributed to the formation of ordered mesopores, so that the final material possessed a hierarchical porosity with specific surface area between 200 and 580 $m^2.g^{-1}$. While these materials were not exploited in catalysis we suggest they could be good candidates for epoxidation. Utilizing high internal phase emulsions (HIPEs)[249,250] as sacrificial templates, Debecker *et al*. recently proposed the synthesis of three-level micro-/meso-/macroporous self-standing Ti–SiO_2 monoliths (Figure 11b).[251] Titanium isopropoxide was pre-hydrolyzed in acidic conditions and polycondensed in the emulsion with pre-hydrolyzed TEOS. Ti atoms could be homogeneously incorporated in the silica matrix with a high dispersion (XPS, UV-vis). This catalyst, coined "SiTi(HIPE)", possessed a macrocellular structure associated with high void fractions (*ca.* 85 %) and high specific surface areas (*ca.* 1000 $m^2.g^{-1}$). It was highly active in batch reactors after grinding of the monolith into powder (up to 1.4 × 10^{-1} s^{-1} TOF for the conversion of cyclohexene with CHP at 90°C). Moving further, cylindrical monoliths were directly implemented in the continuous flow epoxidation of cyclohexene in toluene and with CHP as the oxidant. At 90°C, the CHP conversion reached 66% (with 90% epoxide selectivity) when setting the contact time at 2h.

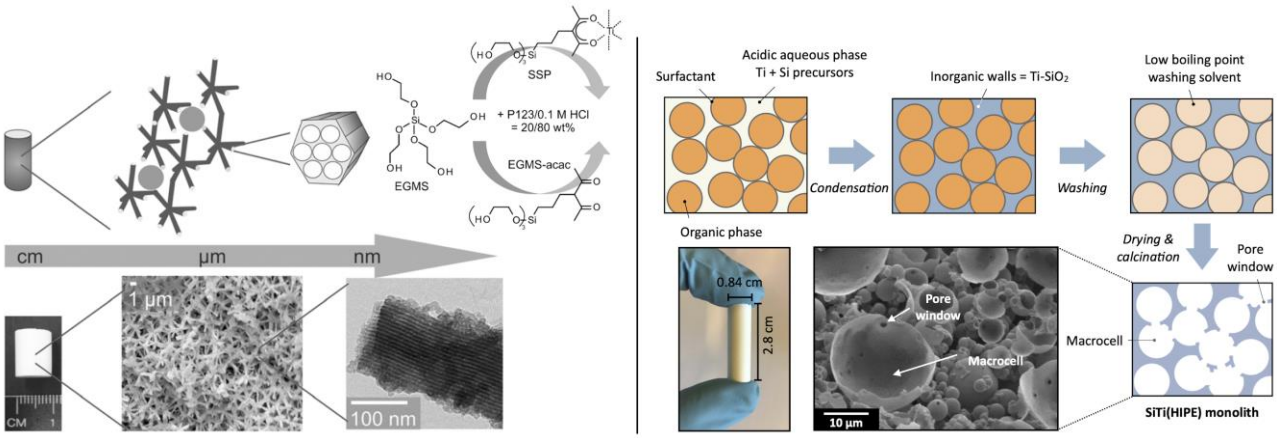

Figure 11. Left: preparation of Ti–SiO_2 monoliths under aqueous conditions starting from a single source Ti precursor (SSP) and tetrakis(2-hydroxyethoxy)silane (EGMS) in the presence of Pluronic P123.[248] Adapted with permission from

reference [248]. Copyright 2014 Wiley-VCH Verlag GmbH & Co. KGaA. Right: formation mechanism of SiTi(HIPE) monoliths using high internal phase emulsions (HIPEs) as template.[251]

3.3.2.2. Use of dedicated processing techniques for synthesis and drying

The processing conditions can also be carefully selected to help tailoring the catalyst properties, especially its texture. To avoid pore shrinkage (especially when the synthesis is done in hydrolytic conditions, in the absence of templating agent), one possibility is to suppress the effect that water exerts during drying due to its high surface tension. Thus, a well-known strategy is to operate the drying under supercritical conditions. Replacing water by supercritical CO_2 – which can then be easily removed from the pores without causing pore collapse – is the way to form highly porous materials coined "aerogels".[252] The technique of aerogel synthesis is well mastered and the scholarly literature in this field, including for heterogeneous catalysis preparation, is abundant and has been reviewed extensively.[253–255] Here, we simply want to mention that Ti-SiO_2 epoxidation catalysts with tailored texture can be obtained by sol-gel chemistry coupled with supercritical drying.[58,210,256–258] For example, Ti–SiO_2 aerogels prepared by Baiker *et al.* are among the most active amorphous epoxidation catalysts (*e.g.* 3.9×10^{-1} s^{-1} TOF for 2-cyclohexen-1-ol conversion with TBHP at 90°C).[82]

Going back to the cases where a sacrificial pore-generating agent is used to create tailored pores (*e.g.* with surfactant micelles, emulsions, etc.), it is important to realize that the catalyst final texture is influenced by the stability of the interactions between the inorganic and organic phases upon condensation and ageing of the gel. Indeed, during these steps, the system spontaneously evolves towards a thermodynamic equilibrium which, in the presence of weak interactions, may correspond to a complete phase separation that eventually compromises the formation of calibrated pores. It can be interesting to try and control these aspects by using peculiar processing conditions.

For example, the fast-drying conditions used the aerosol-assisted sol-gel process can be advantageously used to quench the system before it reaches the thermodynamic equilibrium, thus allowing a tuning of the porosity under various compositions while maintaining high levels of metal dispersion and homogeneity.[187] Recently, hierarchically porous Ti–SiO_2 catalysts were obtained by aerosol -assisted sol-gel, utilizing a combination of TPA^+ cations and Pluronic F127 as templates (Figure 12, see also Figure 9a).[228] Notably, it was demonstrated that by increasing the TPA^+/(Si + Ti) ratio, the system evolved from regularly organized F127 micelles (Figure 12a) towards a partial phase separation assigned to the onset of spinodal decomposition (Figure 12b–c). In the former case, mesostructured Ti–SiO_2 catalysts possessing mesopores with a uniform pore size of *ca.* 15 nm (640 $m^2.g^{-1}$ SSA) were obtained, whereas in the latter case, meso-/macroporous (*ca.* 200 nm macropores, 620 $m^2.g^{-1}$ SSA) Ti–SiO_2 microparticles were formed. Alternatively, macropores can be created through hard templating, as it was shown with polystyrene or polymethyl methacrylate polymer beads (see one example in Figure 9b). The hierarchical Ti–SiO_2 catalysts showed much higher catalytic activity for the epoxidation of cyclohexene with CHP compared to TS-1 (TOF values at 90°C up to

3.5×10^{-2} s^{-1} *vs.* 1.1×10^{-2} s^{-1} for TS-1). In addition to the excellent Ti dispersion offered by the aerosol-assisted sol-gel process (see Section 3.3.1), such high performance was ascribed to the presence of accessible meso- and macro-pores, creating new entry ways for reactants and products.

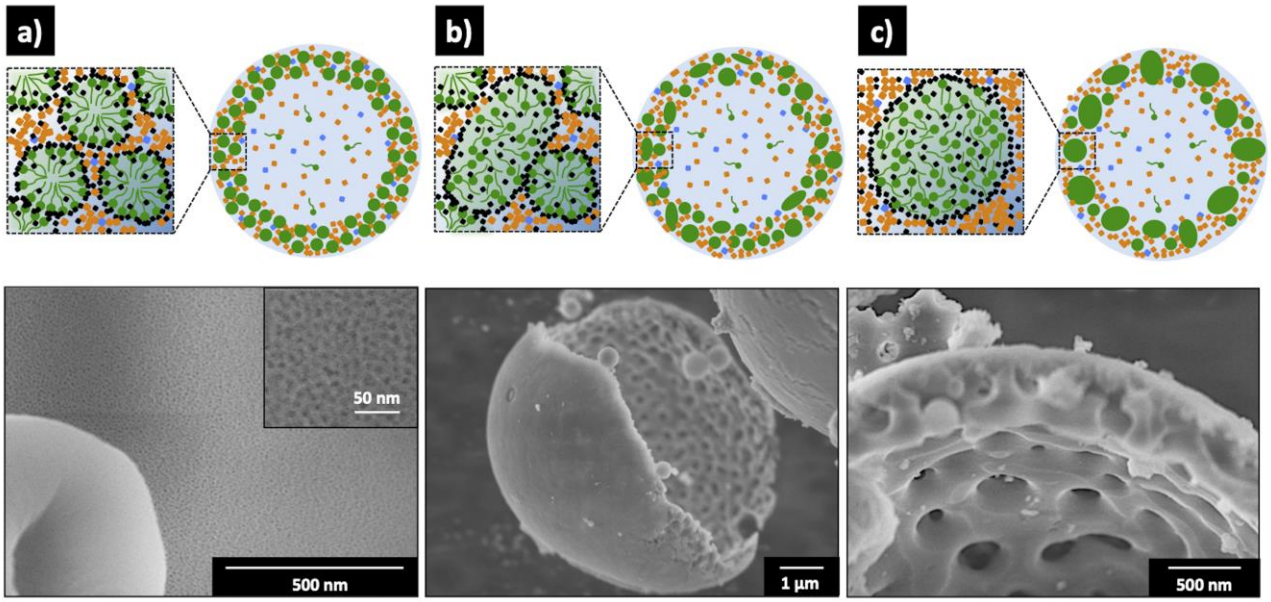

Figure 12. Schematic representation of the aerosol-assisted sol-gel method used for the preparation of hierarchically porous Ti–SiO_2. The porosity was controlled by increasing the TPA^+ to (Si + Ti) molar ratio, which allowed moving from a mesoporous material formed by a simple evaporation-induced self-assembly (EISA) mechanism (a) to a meso-/macroporous solid resulting from a phase separation mechanism (b–c). SEM images of the corresponding materials are shown on the lower side of the figure.[228]

Using a similar approach, Alonso *et al.* fabricated mesoporous Ti–SiO_2 in the presence of chitin nanorods as template and starting from siloxane oligomers and $Ti(O^iPr)_2(acac)_2$ monomers as precursors.[259] The catalysts exhibited pore volume fractions increasing from 0.10 to 0.44 when incorporating larger amounts of chitin, while the S_{BET} increased from 70 to 445 $m^2.g^{-1}$. The pore size was in the 5–6 nm range, in good agreement with the size of the chitin nanorods. These materials showed excellent productivities in sulfoxidation reactions; we surmise that these materials could be excellent catalysts in olefin epoxidation.

3.3.2.3. Utilization of non-hydrolytic synthesis routes

In NHSG methods (see also Section 3.3.1), water is absent from the synthesis medium, and the synthesis is carried out in organic conditions, with organic oxygen-donors.[213] Due to the low tensile strength of the organic solvent, the liquid phase can be easily removed upon drying without impacting the pore network of the gel.[232,233] In these conditions, mesoporous xerogels are formed and the materials usually feature large pore volumes, even in the absence of sacrificial pore-generating agents, simply owing to the liquid phase trapped in the gel.[260] Relatively large pore size distributions are usually obtained. The pore size can be somewhat adjusted by varying the liquid fraction – *e.g.* by adding an organic solvent (CH_2Cl_2, toluene, THF). Also, the reaction time and reaction temperature have a marked impact on the textural properties since these two latter parameters govern the degree

of condensation of the gel and therefore its mechanical resistance.[261] Note that some NHSG protocols can also be carried out in the presence of surfactant to further control the textural properties.[262–264]

Hulea *et al.* have reported the synthesis of a mesoporous Ti–SiO_2 xerogel starting from $SiCl_4$ and $TiCl_4$ as precursors and diisopropyl ether as oxygen donor (alkyl halide elimination route).[265] In this synthesis, the non-hydrolytic condensation reactions took place in CH_2Cl_2. The resulting catalyst possessed pores in the 10–20 nm size range, along with a SSA of 1170 $m^2.g^{-1}$ and a remarkable pore volume of 2.4 $cm^3.g^{-1}$. The catalyst showed a six-fold higher TOF value than TS-1 in the oxidation of dibenzothiophene (DBT) by H_2O_2 (at 60°C), thereby demonstrating that large molecules such as DBT could enter the mesopores of the NHSG catalyst but not the micropores of TS-1. These mesoporous Ti–SiO_2 xerogels exhibited good performance in the epoxidation of cyclic olefins with H_2O_2 (> 64% cyclooctene oxide yield after 6h at 60°C,[265] *ca.* 18% cyclohexene oxide yield after 2h at 60°C[266]). Using CHP as oxidant, Mutin *et al.* reported a >90% cyclohexene oxide yield after 2h at 65°C.[216] In fact, both epoxide yield and initial rate reported in the latter study were found to be nearly as good as those reported by Baiker and co-workers for calcined aerogels.[216] It is important to recall that – in addition to offering a good control on Ti dispersion and a straightforward mean to form materials with open texture – NHSG routes do not require the energy-intensive step of supercritical drying. As such they should be regarded as promising methods for the synthesis of highly effective epoxidation catalysts.

3.3.3. Tackling the susceptibility to water

While water may appear attractive as a solvent (at least for water-soluble substrates), amorphous Ti–SiO_2 catalysts generally deactivate in the presence of water, likewise amorphous Ti supported materials (see Section 3.1). The instability of amorphous Ti–SiO_2 in the presence of water is a well-known issue[80] that dictates the choice of the reaction conditions: amorphous catalysts are generally more active than zeolitic materials with organic hydroperoxides, whereas they show lower performance in the presence of H_2O_2 (Figure 7).[209] In fact, the amorphous nature of the inorganic walls makes these materials less stable in the presence of water,[80] leading to the formation of inert peroxo species[76] (see Scheme 3c) and/or to Ti-leaching. This behavior is further enhanced by the high surface Si–OH density which further promotes the adsorption of water and hence the poisoning of the active sites. High hydrophilicity also contributes to lower the selectivity toward the epoxide product (see Section 3.1).[100] In the case of allylic alcohols, Baiker *et al.*[267] proposed that the epoxidation can occur *via* a "silanol-assisted" mechanism, in which the allylic alcohol molecule is adsorbed by H-bonding to a Si–OH group located in the vicinity of the active Ti site. Such reaction pathway would be responsible for a decrease of regio- and diastereoselectivities that have been respectively observed in the epoxidation of geraniol and cyclohexenol with TBHP in Ti–SiO_2 aerogels.[267] As regard to the epoxidation of geraniol, Guillemot *et al.* reported in 2020 that outer-sphere O-transfer may become competitive with the inner-sphere mechanism (coordination of the allylic alcohol to the Ti center, see Scheme 3b) when using TBHP as oxidant and Ti-siloxy-

polyoxometalates as molecular models for titanosilicates.[268] In the outer-sphere mechanism, a preference for the more nucleophilic 6,7 bond rather than for the 2,3 one is expected and was indeed experimentally observed, thereby accounting for the larger formation of the 6,7-epoxy geraniol over the 2,3-epoxy geraniol (see Scheme 1).

Both activity and selectivity can be improved by increasing the surface hydrophobicity *via* surface silylation or incorporation of organic moieties in the silica framework. Such performance improvement has been observed for hydrophobic Ti–SiO_2 tested in the presence of organic oxidants[213,258,269,270] and even of H_2O_2.[271] Corma and co-workers[269] have reported that a silylated Ti-MCM-41 showed a 93 % conversion of limonene (8h, 70°C) with a 73% epoxide selectivity in the presence of TBHP whereas the pristine Ti-MCM-41 showed only a 56% conversion with 39% selectivity under the same reaction conditions. Similarly, the conversion of cyclohexene (5h, 60°C) was increased from 30% to 75% and the selectivity from 95% to 98% when using this hydrophobic catalyst (Figure 13a). Furthermore, the authors demonstrated that the TON (5h) in the cyclohexene epoxidation with TBHP of silylated Ti-MCM-41 decreased only by 8% when increasing the H_2O concentration in the reaction medium to 10 wt.% (no other solvent added), whereas the selectivity was barely affected (Figure 13b). In comparison, the non-silylated Ti-MCM-41 catalyst suffered a 30% loss in TON.

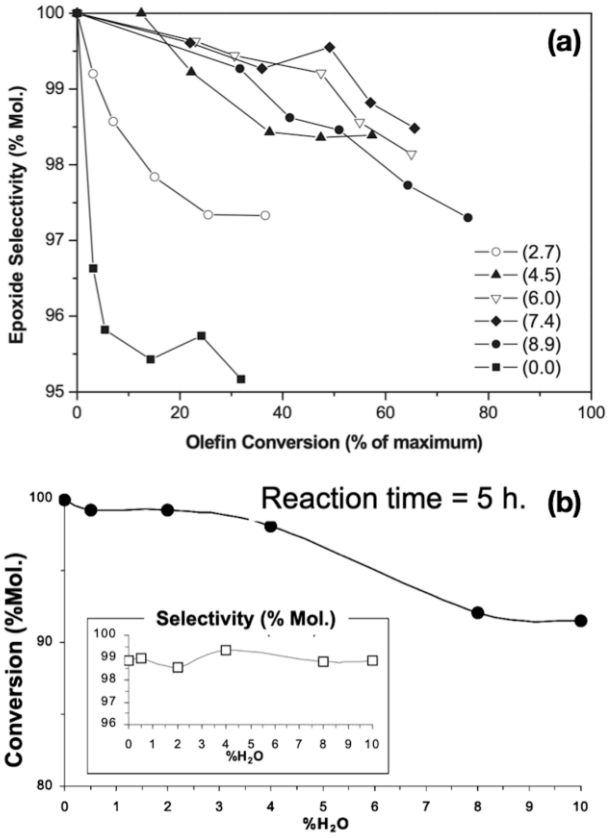

Figure 13. a) Epoxide selectivity as a function of the conversion in the cyclohexene epoxidation with TBHP (0,5 wt.% catalyst, 60°C, 5h) catalyzed by Ti-MCM-41 with different silylation degrees (expressed as the C content in wt.%), b) Effect of water concentration in the reaction medium (in wt.%) on the performance of the silylated Ti-MCM-41 (C content of 8.9 wt.%) catalyst. Adapted with permission from reference [269]. Copyright 2015 Elsevier B.V.

Investigating the effect of a large excess of water in the solvent (25 vol.% H_2O in acetonitrile), the epoxide selectivity of a mesoporous Ti–SiO_2 xerogel prepared by non-hydrolytic routes and tested for the catalytic epoxidation of cyclohexene with H_2O_2 could be increased from 28% to 48% (2h, 60°C) by grafting methyl groups on the catalyst surface by silanization.[266]

More straightforward, the hydrophobization can be achieved in one-pot during the catalyst preparation. This co-synthesis approach is less time-consuming and more economically relevant than post-synthesis modification. Recently, the one-pot methylation of mesoporous Ti–SiO_2 was achieved by adding methyltrimethoxysilane to the gel precursor solution; this led to more hydrophobic epoxidation catalysts with higher initial reaction rates compared to the non-functionalized catalyst (Figure 14).[272] However, two limitations were pointed out: i) the fraction of well-dispersed Ti decreased when increasing the degree of functionalization (as revealed by UV-vis and XPS analyses), ii) an excess of methyl groups reduced the affinity of H_2O_2 with the too hydrophobic catalyst surface. As a result, it is complicated to highlight a direct effect of surface hydrophobicity in this case. Practically speaking, the methyl loading should remain relatively low to benefit from the positive effect of hydrophobization. In fact, the initial rate of the catalyst having a high methyl functionalization (14 mol.% of methyl groups) showed a much lower initial rate than the other methylated catalysts, and even a lower rate than the non-functionalized catalyst (Figure 14). Similar detrimental effects of excessive surface functionalization were also reported by Baiker and co-workers for hydrophobic Ti–SiO_2 aerogels.[258] In the latter study, the incorporation of hydrophobic moieties was additionally shown to alter the textural properties of the catalyst (specific surface area reduced from 813 to *ca.* 650 $m^2.g^{-1}$).

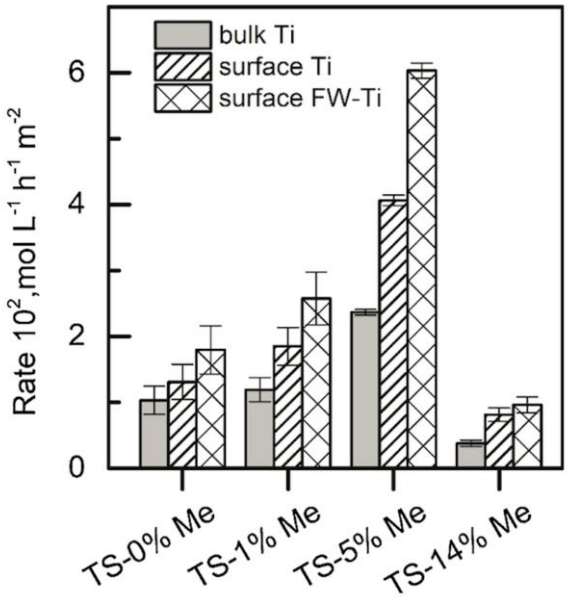

Figure 14. Initial reaction rates normalized by the Ti content for the conversion of cyclooctene with H_2O_2 catalyzed by hydrophobic Ti–SiO_2 prepared in one-pot. "Bulk Ti" from ICP-AES, "surface Ti" and "surface framework (FW) Ti" from XPS. Reproduced with permission from reference [272]. Copyright 2019 Elsevier B.V.

Studying mesoporous Ti–SiO_2 xerogels obtained by non-hydrolytic sol-gel, adding 10 or 30 mol.% $MeSiCl_3$ in a co-synthetic approach led to solids with inhomogeneous Ti dispersion (XRD, XPS, UV-vis) and/or lower mesoporous surface area.[266] As a consequence, these hydrophobic catalysts showed no improvement of the catalytic performance compared to the hydrophilic analogous in the epoxidation of cyclohexene with H_2O_2 in the presence of an excess of water. In another study, however, Mutin *et al.* demonstrated that hydrophobic NHSG catalysts prepared in one-pot with a high degree of functionalization performed very well in organic medium for the epoxidation of cyclohexene with CHP at 90°C (TOF $\approx 1.5 \times 10^{-1}$ s^{-1}).[213]

Actually, it appears that the effects of hydrophobization through co-synthetic sol-gel routes are hard to forecast because the presence of the organosilane in the synthesis tends to affect also the texture and the dispersion of the metal which complicates understanding and optimization of these systems.[194,272] To avoid such effect, it was recently proposed to produce methyl-functionalized Ti-SiO_2 catalysts in one pot, through the aerosol-assisted sol-gel process.[273] This straightforward route led to a series of catalysts with very similar textural properties and tunable degree of functionalization. It allowed the authors to unambiguously demonstrate a positive effect of surface hydrophobicity in the epoxidation of cyclooctene with TBHP as oxidant.

4. Conclusions and prospects

As has been concluded by multiple studies discussed in this review, developing efficient epoxidation processes directly relies on our ability to establish innovative catalyst synthesis strategies. The current trends in the research efforts on catalyst design is towards the preparation of catalysts which not only feature good performance (activity, selectivity, stability), but also have a wide substrate scope and are easy to handle in practical applications. The majority of this review has discussed the role of catalyst preparation to achieve improved performance thanks to upgraded physico-chemical properties. In many cases, it was observed that texture plays the key role as it determines both the number of active sites and their accessibility to substrate and oxidant molecules. Another parameter of importance is the Ti speciation, especially in amorphous titanosilicate and supported catalysts.

Looking forward, some of the synthesis strategies discussed in here have a particularly bright forecast. Zeolite synthesis research is progressing at a fast pace,[274,275] discovering new topologies and new ways to control Ti-content and Ti location. Importantly, the development of hierarchically porous zeolites will open avenues of progress, allowing to expand the scope of zeolite-based epoxidation reactions. While the synthesis of zeolite nanocrystal catalysts often gives access to high catalytic performance, owing to the large surface-to-volume ratio, the size of these nanoobjects imposes further work on the formation of larger particles (i.e. aggregates of nanocrystals) which can be manipulated, recovered, and recycled more easily and more safely. In the field of supported catalysts, surface organometallic chemistry (SOMC)[276] is identified as a powerful toolbox for the molecular-level understanding of the catalytic mechanism and for the further optimization of the

active sites. For the preparation of amorphous titanosilicate catalysts, sol-gel chemists are already greatly mastering the art of creating advantageous textural properties, using sacrificial templates (micelles, polymers, emulsions, etc.) and dedicated drying methods.[277] We suggest that further important progress can be expected from the development of methods that allow controlling the Ti dispersion in amorphous titanosilicates, and by consequence the Ti speciation at the surface of the catalyst. In this respect, the kinetic control offered by aerosol-assisted sol-gel and non-hydrolytic sol-gel routes provides significant opportunities.[187,229]

An important outlook for the preparation of more advanced titanosilicate epoxidation catalysts is on the preparation of shaped catalytic objects, including 2D materials, self-standing porous monoliths, tubular structure, etc. These could pave the way to efficient continuous flow processes, possibly concatenated in a cascade fashion with other reactions, or with other unit operations such as purification.[278–280] In a move toward process intensification, a focus could be put on reactor design, so that the catalyst morphology is envisaged and optimized directly as a function of its future integration in a given process configuration.

In the near future, progress can be expected from a better understanding of the role of surface polarity.[281,282] Hydrophobization of hydrophilic titanosilicate catalysts has undoubtedly shown to have a significant impact on catalyst behavior, and some results are promising, in particular for boosting the catalyst epoxidation selectivity. Yet for many catalyst preparation methods, unpredictable effects of the incorporation of hydrophobic groups on Ti speciation and on texture make these studies difficult to interpret and further work is required to decipher the unifying principles of catalyst improvement via hydrophobization. We surmise that post-synthesis modification (e.g. using fluoride treatments), or the fine tuning of thermal treatment (e.g. to tailor the degree of silanol condensation) would help unravelling the underlying mechanisms that govern these surface effects.

Finally, hybrid catalysis – combining more than one type of catalyst (homogeneous, heterogeneous or enzymatic) – is considered as an emerging field of investigation, in which epoxidation reactions catalyzed by titanosilicate catalysts may have an important role to play. Although the frontiers between the different types of catalysts are theoretically well-defined, recent progresses on epoxidation catalysts show that this should be considered with some flexibility: for example, metal complexes can be immobilized onto heterogeneous supports – either covalently or through ion exchange and coordination bond – thereby forming molecularly well-defined heterogeneous catalysts[211,276,283–285] that may find application in the industrial production of valuable products, such as bisepoxides (*e.g.* divinylbenzene dioxide[286,287]) used in epoxy resins. Also, pristine chemical space could be explored – also in the field of epoxidation – with the help of hybrid chemo-enzymatic heterogeneous catalysts.[288] While a first example of hybrid chemo-enzymatic heterogeneous catalysis was recently reported for the epoxidation of allyl alcohol using in-situ generated hydrogen peroxide,[191] we suggest that the most relevant developments that can be expected is in the field of organic synthesis towards high added-value – possibly chirally pure – chemicals.

Acknowledgements

Authors acknowledge the 'Communauté française de Belgique' for the financial support through the ARC programme (15/20-069). D.P. Debecker thanks the Francqui Foundation for his "Francqui Research Professor" chair. V. Smeets is thankful to F.R.S.–F.N.R.S. for his FRIA PhD grant.

Keywords

Mesoporous catalysts, olefin epoxidation, sol-gel chemistry, titanosilicate, TS-1 zeolite

References

[1] J. N. Armor, *Catal. Today* **2011**, *163*, 3–9.
[2] G. Centi, S. Perathoner, *Catal. Today* **2003**, *77*, 287–297.
[3] R. A. Sheldon, *J. R. Soc. Interface* **2016**, *13*, 20160087.
[4] H. C. Erythropel, J. B. Zimmerman, T. M. de Winter, L. Petitjean, F. Melnikov, C. H. Lam, A. W. Lounsbury, K. E. Mellor, N. Z. Janković, Q. Tu, et al., *Green Chem.* **2018**, *20*, 1929–1961.
[5] P. T. Anastas, M. M. Kirchhoff, T. C. Williamson, *Appl. Catal. Gen.* **2001**, *221*, 3–13.
[6] I. Pálinkó, in *Green Chem.* (Eds.: B. Török, T. Dransfield), Elsevier, **2018**, pp. 415–447.
[7] A. S. Sharma, V. S. Sharma, H. Kaur, R. S. Varma, *Green Chem.* **2020**, *22*, 5902–5936.
[8] F. Wattimena, H. P. Wulff, *A Process for Epoxidizing Olefins with Organic Hydroperoxides*, **1971**, GB1249079A.
[9] M. Taramasso, G. Perego, B. Notari, *Preparation of Porous Crystalline Synthetic Material Comprised of Silicon and Titanium Oxides*, **1983**, US4410501A.
[10] M. G. Clerici, G. Bellussi, U. Romano, *J. Catal.* **1991**, *129*, 159–167.
[11] A. Forlin, P. Tegon, G. Paparatto, *Process for the Continuous Production of an Olefinic Oxide*, **2006**, US7138534B2.
[12] U. Romano, M. Ricci, in *Liq. Phase Oxid. Heterog. Catal.*, John Wiley & Sons, Ltd, **2013**, pp. 451–506.
[13] J. Tsuji, T. Omae, *Process for Producing Propylene Oxide*, **2003**, US6639086B2.
[14] "Sumitomo Chemical Signs Technology License Agreement for Propylene Oxide with One of India's Leading Government-owned Oil Companies," can be found under https://www.sumitomo-chem.co.jp/english/news/detail/20190819e.html, **2021**.
[15] J. Tsuji, J. Yamamoto, M. Ishino, N. Oku, *Development of New Propylene Oxide Process.* Paper translated from R&D Report "Sumimoto Kagaku", vol. 2006-I
[16] R. Bai, Y. Song, R. Bai, J. Yu, *Adv. Mater. Interfaces* **2021**, *8*, 2001095.
[17] G. Bellussi, R. Millini, in *Struct. React. Met. Zeolite Mater.* (Eds.: J. Pérez Pariente, M. Sánchez-Sánchez), Springer International Publishing, Cham, **2018**, pp. 1–52.
[18] M. Moliner, A. Corma, *Microporous Mesoporous Mater.* **2014**, *189*, 31–40.
[19] J. Přech, *Catal. Rev.* **2018**, *60*, 71–131.
[20] G. Sienel, R. Rieth, K. T. Rowbottom, in *Ullmanns Encycl. Ind. Chem.*, American Cancer Society, **2000**.
[21] M. Ghanta, B. Subramaniam, H.-J. Lee, D. H. Busch, *AIChE J.* **2013**, *59*, 180–187.
[22] "Propylene Oxide Product Life Cycle | Technologies," can be found under https://www.gdch.de/fileadmin/downloads/Netzwerk_und_Strukturen/Fachgruppen/Seniorexperten/PDF/Tagungen/4_SEC_Jahrestreffen/4SECJT_Nees2.pdf, **2021**.
[23] J. C. Zomerdijk, M. W. Hall, *Catal. Rev.* **1981**, *23*, 163–185.
[24] F. Cavani, G. Centi, S. Perathoner, F. Trifirò, *Sustainable Industrial Chemistry: Principles, Tools and Industrial Examples*, Wiley, **2009**.
[25] S. T. Oyama, *Mechanisms in Homogeneous and Heterogeneous Epoxidation Catalysis*, Elsevier, **2011**.
[26] G. Grigoropoulou, J. H. Clark, J. A. Elings, *Green Chem.* **2003**, *5*, 1–7.
[27] H. H. Voge, C. R. Adams, in *Adv. Catal.* (Eds.: D.D. Eley, H. Pines, P.B. Weisz), Academic Press, **1967**, pp. 151–221.
[28] T. E. Jones, R. Wyrwich, S. Böcklein, E. A. Carbonio, M. T. Greiner, A. Yu. Klyushin, W. Moritz, A. Locatelli, T. O. Menteş, M. A. Niño, et al., *ACS Catal.* **2018**, *8*, 3844–3852.
[29] A. J. F. van Hoof, I. A. W. Filot, H. Friedrich, E. J. M. Hensen, *ACS Catal.* **2018**, *8*, 11794–11800.
[30] J. Lu, J. J. Bravo-Suárez, A. Takahashi, M. Haruta, S. T. Oyama, *J. Catal.* **2005**, *232*, 85–95.
[31] J. Teržan, M. Huš, B. Likozar, P. Djinović, *ACS Catal.* **2020**, *10*, 13415–13436.
[32] T. Katsuki, K. B. Sharpless, *J. Am. Chem. Soc.* **1980**, *102*, 5974–5976.
[33] W. Zhang, J. L. Loebach, S. R. Wilson, E. N. Jacobsen, *J. Am. Chem. Soc.* **1990**, *112*, 2801–2803.
[34] J. J. Li, in *Name React. Collect. Detail. Mech. Synth. Appl. Fifth Ed.* (Ed.: J.J. Li), Springer International

Publishing, Cham, **2014**, pp. 552–554.
[35] F. Peter Guengerich, *Arch. Biochem. Biophys.* **2003**, *409*, 59–71.
[36] A. A. Spector, *J. Lipid Res.* **2009**, *50*, S52–S56.
[37] I. Fleming, *Pharmacol. Rev.* **2014**, *66*, 1106–1140.
[38] A. D. N. Vaz, D. F. McGinnity, M. J. Coon, *Proc. Natl. Acad. Sci.* **1998**, *95*, 3555–3560.
[39] N. J. Turner, *Nat. Chem. Biol.* **2009**, *5*, 567–573.
[40] U. T. Bornscheuer, G. W. Huisman, R. J. Kazlauskas, S. Lutz, J. C. Moore, K. Robins, *Nature* **2012**, *485*, 185–194.
[41] E. T. Farinas, M. Alcalde, F. Arnold, *Tetrahedron* **2004**, *60*, 525–528.
[42] S. Peter, M. Kinne, R. Ullrich, G. Kayser, M. Hofrichter, *Enzyme Microb. Technol.* **2013**, *52*, 370–376.
[43] J. Carro, A. González-Benjumea, E. Fernández-Fueyo, C. Aranda, V. Guallar, A. Gutiérrez, A. T. Martínez, *ACS Catal.* **2019**, *9*, 6234–6242.
[44] X. Huali, F. Yongxian, Z. Chunhui, D. Zexue, M. Enze, G. Zhonghua, L. Xiaonian, *Chem. Biochem. Eng. Q.* **2008**, *22*, 25–39.
[45] D. A. Ruddy, T. D. Tilley, *J. Am. Chem. Soc.* **2008**, *130*, 11088–11096.
[46] W. Lueangchaichaweng, L. Li, Q.-Y. Wang, B.-L. Su, C. Aprile, P. P. Pescarmona, *Catal. Today* **2013**, *203*, 66–75.
[47] C. Anand, P. Srinivasu, G. P. Mane, S. N. Talapaneni, M. R. Benzigar, S. Vishnu Priya, S. S. Al-deyab, Y. Sugi, A. Vinu, *Microporous Mesoporous Mater.* **2013**, *167*, 146–154.
[48] D. Lahcene, A. Choukchou-Braham, C. Kappenstein, L. Pirault-Roy, *J. Sol-Gel Sci. Technol.* **2012**, *64*, 637–642.
[49] A. Ramanathan, H. Zhu, R. Maheswari, B. Subramaniam, *Microporous Mesoporous Mater.* **2018**, *261*, 158–163.
[50] D. T. Bregante, D. W. Flaherty, *J. Am. Chem. Soc.* **2017**, *139*, 6888–6898.
[51] V. Sydorchuk, O. Makota, S. Khalameida, L. Bulgakova, J. Skubiszewska-Zięba, R. Leboda, V. Zazhigalov, *J. Therm. Anal. Calorim.* **2012**, *108*, 1001–1008.
[52] E. E. Stangland, K. B. Stavens, R. P. Andres, W. N. Delgass, *J. Catal.* **2000**, *191*, 332–347.
[53] J. E. van den Reijen, S. Kanungo, T. A. J. Welling, M. Versluijs-Helder, T. A. Nijhuis, K. P. de Jong, P. E. de Jongh, *J. Catal.* **2017**, *356*, 65–74.
[54] D. Gajan, K. Guillois, P. Delichère, J.-M. Basset, J.-P. Candy, V. Caps, C. Coperet, A. Lesage, L. Emsley, *J. Am. Chem. Soc.* **2009**, *131*, 14667–14669.
[55] Q. Yang, C. Copéret, C. Li, J.-M. Basset, *New J. Chem.* **2003**, *27*, 319–323.
[56] J. K. F. Buijink, J.-P. Lange, A. N. R. Bos, A. D. Horton, F. G. M. Niele, in *Mech. Homog. Heterog. Epoxidation Catal.* (Ed.: S.T. Oyama), Elsevier, Amsterdam, **2008**, pp. 355–371.
[57] G. Ming-Xing, G. Hong-Chen, W. Xiang-Sheng, G. Wei-Min, *Chin. J. Chem.* **2005**, *23*, 471–473.
[58] R. Hutter, T. Mallat, D. Dutoit, A. Baiker, *Top. Catal.* **1996**, *3*, 421–436.
[59] D. Srinivas, P. Manikandan, S. C. Laha, R. Kumar, P. Ratnasamy, *J. Catal.* **2003**, *217*, 160–171.
[60] W. Panyaburapa, T. Nanok, J. Limtrakul, *J. Phys. Chem. C* **2007**, *111*, 3433–3441.
[61] S. Bordiga, F. Boscherini, S. Coluccia, F. Genonic, C. Lamberti, G. Leofanti, L. Marchese, G. Petrini, G. Vlaic, A. Zecchina, *Catal. Lett.* **1994**, *26*, 195–208.
[62] G. Berlier, V. Crocellà, M. Signorile, E. Borfecchia, F. Bonino, S. Bordiga, in *Struct. React. Met. Zeolite Mater.* (Eds.: J. Pérez Pariente, M. Sánchez-Sánchez), Springer International Publishing, Cham, **2018**, pp. 91–154.
[63] B. Erdem, R. A. Hunsicker, G. W. Simmons, E. D. Sudol, V. L. Dimonie, M. S. El-Aasser, *Langmuir* **2001**, *17*, 2664–2669.
[64] B. M. Reddy, B. Chowdhury, P. G. Smirniotis, *Appl. Catal. Gen.* **2001**, *211*, 19–30.
[65] M. R. Boccuti, K. M. Rao, A. Zecchina, G. Leofanti, G. Petrini, in *Stud. Surf. Sci. Catal.* (Eds.: C. Morterra, A. Zecchina, G. Costa), Elsevier, **1989**, pp. 133–144.
[66] X. Gao, S. R. Bare, J. L. G. Fierro, M. A. Banares, I. E. Wachs, *J. Phys. Chem. B* **1998**, *102*, 5653–5666.
[67] E. Astorino, J. B. Peri, R. J. Willey, G. Busca, *J. Catal.* **1995**, *157*, 482–500.
[68] S. Klein, S. Thorimbert, W. F. Maier, *J. Catal.* **1996**, *163*, 476–488.
[69] M. Schraml-Marth, K. L. Walther, A. Wokaun, B. E. Handy, A. Baiker, *J. Non-Cryst. Solids* **1992**, *143*, 93–111.
[70] K. Thamaphat, P. Limsuwan, B. Ngotawornchai, *Kasetsart J Nat Sci* **2008**, *42*, 357–361.
[71] P. Ratnasamy, D. Srinivas, H. Knözinger, in (Ed.: B.-A. in Catalysis), Academic Press, **2004**, pp. 1–169.
[72] A. Solé-Daura, T. Zhang, H. Fouilloux, C. Robert, C. M. Thomas, L.-M. Chamoreau, J. J. Carbó, A. Proust, G. Guillemot, J. M. Poblet, *ACS Catal.* **2020**, *10*, 4737–4750.
[73] P. Jiménez-Lozano, I. Y. Skobelev, O. A. Kholdeeva, J. M. Poblet, J. J. Carbó, *Inorg. Chem.* **2016**, *55*, 6080–6084.
[74] M. G. Clerici, *Top. Catal.* **2001**, *15*, 257–263.
[75] C. P. Gordon, H. Engler, A. S. Tragl, M. Plodinec, T. Lunkenbein, A. Berkessel, J. H. Teles, A.-N. Parvulescu, C. Copéret, *Nature* **2020**, *586*, 708–713.
[76] M. G. Clerici, *Kinet. Catal.* **2015**, *56*, 450–455.
[77] N. A. Grosso-Giordano, A. S. Hoffman, A. Boubnov, D. W. Small, S. R. Bare, S. I. Zones, A. Katz, *J. Am. Chem.*

Soc. **2019**, *141*, 7090–7106.
[78] R. Murugavel, H. W. Roesky, *Angew. Chem. Int. Ed.* **1997**, *36*, 477–479.
[79] F. Bonino, A. Damin, G. Ricchiardi, M. Ricci, G. Spanò, R. D'Aloisio, A. Zecchina, C. Lamberti, C. Prestipino, S. Bordiga, *J. Phys. Chem. B* **2004**, *108*, 3573–3583.
[80] G. Deo, A. M. Turek, I. E. Wachs, D. R. C. Huybrechts, P. A. Jacobs, *Zeolites* **1993**, *13*, 365–373.
[81] A. O. Bouh, G. L. Rice, S. L. Scott, *J. Am. Chem. Soc.* **1999**, *121*, 7201–7210.
[82] C. Beck, T. Mallat, T. Bürgi, A. Baiker, *J. Catal.* **2001**, *204*, 428–439.
[83] L. Fang, B. Albela, B. Yang, Y. Zheng, P. Wu, M. He, L. Bonneviot, *Langmuir* **2018**, *34*, 12713–12722.
[84] G. Xiong, Y. Cao, Z. Guo, Q. Jia, F. Tian, L. Liu, *Phys. Chem. Chem. Phys.* **2015**, *18*, 190–196.
[85] M. H. Zahedi-Niaki, M. P. Kapoor, S. Kaliaguine, *J. Catal.* **1998**, *177*, 231–239.
[86] N. A. Grosso-Giordano, C. Schroeder, A. Okrut, A. Solovyov, C. Schöttle, W. Chassé, N. Marinković, H. Koller, S. I. Zones, A. Katz, *J. Am. Chem. Soc.* **2018**, *140*, 4956–4960.
[87] D. T. Bregante, N. E. Thornburg, J. M. Notestein, D. W. Flaherty, *ACS Catal.* **2018**, *8*, 2995–3010.
[88] D. H. Wells, A. M. Joshi, W. N. Delgass, K. T. Thomson, *J. Phys. Chem. B* **2006**, *110*, 14627–14639.
[89] D. T. Bregante, J. Z. Tan, R. L. Schultz, E. Z. Ayla, D. S. Potts, C. Torres, D. W. Flaherty, *ACS Catal.* **2020**, *10*, 10169–10184.
[90] H. P. Wulff, F. Wattimena, *Olefin Epoxidation*, **1983**, US4367342A.
[91] Y.-Z. Han, E. Morales, R. G. Gastinger, K. M. Carroll, *Heterogeneous Epoxidation Catalyst*, **2000**, US6114552A.
[92] R. A. Sheldon, J. Dakka, *Catal. Today* **1994**, *19*, 215–245.
[93] K.-T. Li, I.-C. Chen, *Ind. Eng. Chem. Res.* **2002**, *41*, 4028–4034.
[94] G. P. Chiusoli, P. M. Maitlis, Eds., *Metal-Catalysis in Industrial Organic Processes*, Royal Society of Chemistry, **2006**.
[95] N. Tsunoji, M. V. Opanasenko, M. Kubů, J. Čejka, H. Nishida, S. Hayakawa, Y. Ide, M. Sadakane, T. Sano, *ChemCatChem* **2018**, *10*, 2536–2540.
[96] M. Fukuda, N. Tsunoji, Y. Yagenji, Y. Ide, S. Hayakawa, M. Sadakane, T. Sano, *J. Mater. Chem. A* **2015**, *3*, 15280–15291.
[97] F. Chiker, F. Launay, J. P. Nogier, J. L. Bonardet, *Green Chem.* **2003**, *5*, 318–322.
[98] C.-C. Chang, J.-F. Lee, S. Cheng, *J. Mater. Chem. A* **2017**, *5*, 15676–15687.
[99] A. Okrut, M. Aigner, C. Schöttle, N. A. Grosso-Giordano, S.-J. Hwang, X. Ouyang, S. Zones, A. Katz, *Dalton Trans.* **2018**, *47*, 15082–15090.
[100] T. Blasco, A. Corma, M. T. Navarro, J. P. Pariente, *J. Catal.* **1995**, *156*, 65–74.
[101] J. M. Fraile, J. I. García, J. A. Mayoral, E. Vispe, D. R. Brown, M. Naderi, *Chem. Commun.* **2001**, *0*, 1510–1511.
[102] M. Aigner, N. A. Grosso-Giordano, A. Okrut, S. Zones, A. Katz, *React. Chem. Eng.* **2017**, *2*, 842–851.
[103] M. Aigner, N. A. Grosso-Giordano, C. Schöttle, A. Okrut, S. Zones, A. Katz, *React. Chem. Eng.* **2017**, *2*, 852–861.
[104] F. Bini, C. Rosier, R. P. Saint-Arroman, E. Neumann, C. Dablemont, A. de Mallmann, F. Lefebvre, G. P. Niccolai, J.-M. Basset, M. Crocker, et al., *Organometallics* **2006**, *25*, 3743–3760.
[105] X. Hou, Z. Wang, C. Fang, T. Li, S. Pan, *Appl. Surf. Sci.* **2018**, *455*, 561–569.
[106] J. M. Fraile, N. García, J. A. Mayoral, F. G. Santomauro, M. Guidotti, *ACS Catal.* **2015**, *5*, 3552–3561.
[107] P. Wu, T. Tatsumi, T. Komatsu, T. Yashima, *Chem. Mater.* **2002**, *14*, 1657–1664.
[108] Z. Luan, E. M. Maes, P. A. W. van der Heide, D. Zhao, R. S. Czernuszewicz, L. Kevan, *Chem. Mater.* **1999**, *11*, 3680–3686.
[109] K. Su, T. D. Tilley, *Chem. Mater.* **1997**, *9*, 588–595.
[110] J. Jarupatrakorn, T. D. Tilley, *J. Am. Chem. Soc.* **2002**, *124*, 8380–8388.
[111] S. Sakugawa, K. Wada, M. Inoue, *J. Catal.* **2010**, *275*, 280–287.
[112] I. V. Yudanov, P. Gisdakis, C. D. Valentin, N. Rösch, *Eur. J. Inorg. Chem.* **1999**, *1999*, 2135–2145.
[113] Y. Guo, S.-J. Hwang, A. Katz, *Mol. Catal.* **2019**, *477*, 110509.
[114] J. M. Fraile, J. I. García, J. A. Mayoral, E. Vispe, *J. Catal.* **2001**, *204*, 146–156.
[115] E. Jorda, A. Tuel, R. Teissier, J. Kervennal, *J. Catal.* **1998**, *175*, 93–107.
[116] C. W. Yoon, K. F. Hirsekorn, M. L. Neidig, X. Yang, T. D. Tilley, *ACS Catal.* **2011**, *1*, 1665–1678.
[117] Y. Yu, Z. Tang, J. Wang, R. Wang, Z. Chen, H. Liu, K. Shen, X. Huang, Y. Liu, M. He, *J. Catal.* **2020**, *381*, 96–107.
[118] J. M. Fraile, J. I. García, J. A. Mayoral, E. Vispe, *J. Catal.* **2000**, *189*, 40–51.
[119] R. L. Brutchey, D. A. Ruddy, L. K. Andersen, T. D. Tilley, *Langmuir ACS J. Surf. Colloids* **2005**, *21*, 9576–9583.
[120] M. G. Clerici, P. Ingallina, *J. Catal.* **1993**, *140*, 71–83.
[121] S.-K. Kim, B. M. Reddy, S.-E. Park, *Ind. Eng. Chem. Res.* **2018**, *57*, 3567–3574.
[122] D. A. Ruddy, R. L. Brutchey, T. D. Tilley, *Top. Catal.* **2008**, *48*, 99–106.
[123] P. E. Sinclair, C. R. A. Catlow, *J. Phys. Chem. B* **1999**, *103*, 1084–1095.
[124] E. H. Aish, M. Crocker, F. T. Ladipo, *J. Catal.* **2010**, *273*, 66–72.
[125] T. Kamegawa, N. Suzuki, K. Tsuji, J. Sonoda, Y. Kuwahara, K. Mori, H. Yamashita, *Catal. Today* **2011**, *175*,

393–397.
[126] M. A. Ardagh, D. T. Bregante, D. W. Flaherty, J. M. Notestein, *ACS Catal.* **2020**, *10*, 13008–13018.
[127] B. Notari, *Stud. Surf. Sci. Catal.* **1988**, *37*, 413–425.
[128] M. Hartmann, A. G. Machoke, W. Schwieger, *Chem. Soc. Rev.* **2016**, *45*, 3313–3330.
[129] A. Thangaraj, M. J. Eapen, S. Sivasanker, P. Ratnasamy, *Zeolites* **1992**, *12*, 943–950.
[130] H. L. Chen, S. W. Li, Y. M. Wang, *J. Mater. Chem. A* **2015**, *3*, 5889–5900.
[131] J. S. Reddy, S. Sivasanker, P. Ratnasamy, *J. Mol. Catal.* **1992**, *71*, 373–381.
[132] R. Millini, E. Previde Massara, G. Perego, G. Bellussi, *J. Catal.* **1992**, *137*, 497–503.
[133] B. Wang, H. Xu, Z. Zhu, Y. Guan, P. Wu, *Catal. Sci. Technol.* **2019**, *9*, 1857–1866.
[134] M. A. Camblor, A. Corma, A. Martínez, J. Pérez-Pariente, *J. Chem. Soc. Chem. Commun.* **1992**, *0*, 589–590.
[135] P. Wu, T. Tatsumi, T. Komatsu, T. Yashima, *J. Phys. Chem. B* **2001**, *105*, 2897–2905.
[136] P. Wu, H. Xu, L. Xu, Y. Liu, M. He, in *MWW-Type Titanosilicate Synth. Struct. Modif. Catal. Appl. Green Oxid.* (Eds.: P. Wu, H. Xu, L. Xu, Y. Liu, M. He), Springer Berlin Heidelberg, Berlin, Heidelberg, **2013**, pp. 35–61.
[137] Y. J. He, G. S. Nivarthy, F. Eder, K. Seshan, J. A. Lercher, *Microporous Mesoporous Mater.* **1998**, *25*, 207–224.
[138] K. Na, C. Jo, J. Kim, W.-S. Ahn, R. Ryoo, *ACS Catal.* **2011**, *1*, 901–907.
[139] N. Wilde, J. Přech, M. Pelz, M. Kubů, J. Čejka, R. Gläser, *Catal. Sci. Technol.* **2016**, *6*, 7280–7288.
[140] Y. Zuo, M. Liu, T. Zhang, C. Meng, X. Guo, C. Song, *ChemCatChem* **2015**, *7*, 2660–2668.
[141] M. Shakeri, S. B. Dehghanpour, *Microporous Mesoporous Mater.* **2020**, *298*, 110066.
[142] S. Mintova, J.-P. Gilson, V. Valtchev, *Nanoscale* **2013**, *5*, 6693–6703.
[143] H. Liu, G. Lu, Y. Guo, Y. Guo, J. Wang, *Chem. Eng. J.* **2005**, *108*, 187–192.
[144] D. Trong-On, A. Ungureanu, S. Kaliaguine, *Phys. Chem. Chem. Phys.* **2003**, *5*, 3534–3538.
[145] S. Li, J. Li, M. Dong, S. Fan, T. Zhao, J. Wang, W. Fan, *Chem. Soc. Rev.* **2019**, *48*, 885–907.
[146] J. Wang, L. Xu, K. Zhang, H. Peng, H. Wu, J. Jiang, Y. Liu, P. Wu, *J. Catal.* **2012**, *288*, 16–23.
[147] A. Corma, *Chem. Rev.* **1997**, *97*, 2373–2419.
[148] M. Dusselier, M. E. Davis, *Chem. Rev.* **2018**, *118*, 5265–5329.
[149] J. C. van der Waal, P. Lin, M. S. Rigutto, H. van Bekkum, in *Stud. Surf. Sci. Catal.* (Eds.: H. Chon, S.-K. Ihm, Y.S. Uh), Elsevier, **1997**, pp. 1093–1100.
[150] J. Přech, J. Čejka, *Catal. Today* **2016**, *277*, 2–8.
[151] Y. Jiao, A.-L. Adedigba, Q. He, P. Miedziak, G. Brett, N. F. Dummer, M. Perdjon, J. Liu, G. J. Hutchings, *Catal. Sci. Technol.* **2018**, *8*, 2211–2217.
[152] D. P. Serrano, R. Sanz, P. Pizarro, I. Moreno, *Top. Catal.* **2010**, *53*, 1319–1329.
[153] H. Qu, Y. Ma, B. Li, L. Wang, *Emergent Mater.* **2020**, *3*, 225–245.
[154] S. Guo, Y. Zhang, Y. Ye, J. Song, M. Li, *ACS Omega* **2020**, *5*, 9912–9919.
[155] P. Eliášová, M. Opanasenko, P. S. Wheatley, M. Shamzhy, M. Mazur, P. Nachtigall, W. J. Roth, R. E. Morris, J. Čejka, *Chem. Soc. Rev.* **2015**, *44*, 7177–7206.
[156] Y. Kubota, S. Inagaki, *Top. Catal.* **2015**, *58*, 480–493.
[157] W. Fan, P. Wu, T. Tatsumi, *J. Catal.* **2008**, *256*, 62–73.
[158] J. Přech, P. Eliášová, D. Aldhayan, M. Kubů, *Catal. Today* **2015**, *243*, 134–140.
[159] W. Wu, D. T. Tran, X. Wu, S. C. Oh, M. Wang, H. Chen, L. Emdadi, J. Zhang, E. Schulman, D. Liu, *Microporous Mesoporous Mater.* **2019**, *278*, 414–422.
[160] I. Schmidt, A. Krogh, K. Wienberg, A. Carlsson, M. Brorson, C. J. H. Jacobsen, *Chem. Commun.* **2000**, *0*, 2157–2158.
[161] N. Wilde, M. Pelz, S. G. Gebhardt, R. Gläser, *Green Chem.* **2015**, *17*, 3378–3389.
[162] J. Tekla, K. A. Tarach, Z. Olejniczak, V. Girman, K. Góra-Marek, *Microporous Mesoporous Mater.* **2016**, *233*, 16–25.
[163] G. Xiong, D. Hu, Z. Guo, Q. Meng, L. Liu, *Microporous Mesoporous Mater.* **2018**, *268*, 93–99.
[164] M. Ogura, S. Shinomiya, J. Tateno, Y. Nara, M. Nomura, E. Kikuchi, M. Matsukata, *Appl. Catal. Gen.* **2001**, *219*, 33–43.
[165] Y. Zuo, T. Zhang, M. Liu, Y. Ji, C. Song, X. Guo, *Ind. Eng. Chem. Res.* **2018**, *57*, 512–520.
[166] Q. Du, Y. Guo, P. Wu, H. Liu, Y. Chen, *Microporous Mesoporous Mater.* **2019**, *275*, 61–68.
[167] H. Xin, J. Zhao, S. Xu, J. Li, W. Zhang, X. Guo, E. J. M. Hensen, Q. Yang, C. Li, *J. Phys. Chem. C* **2010**, *114*, 6553–6559.
[168] Z. Han, Y. Shen, X. Qin, F. Wang, X. Zhang, G. Wang, H. Li, *ChemistrySelect* **2019**, *4*, 1618–1626.
[169] S. Park, K. M. Cho, M. H. Youn, J. G. Seo, J. C. Jung, S.-H. Baeck, T. J. Kim, Y.-M. Chung, S.-H. Oh, I. K. Song, *Catal. Commun.* **2008**, *9*, 2485–2488.
[170] R. Sanz, D. P. Serrano, P. Pizarro, I. Moreno, *Chem. Eng. J.* **2011**, *171*, 1428–1438.
[171] K. Möller, B. Yilmaz, R. M. Jacubinas, U. Müller, T. Bein, *J. Am. Chem. Soc.* **2011**, *133*, 5284–5295.
[172] Y. Zhang, K. Zhu, X. Zhou, W. Yuan, *New J. Chem.* **2014**, *38*, 5808–5816.
[173] W. Song, Z. Liu, L. Liu, A. L. Skov, N. Song, G. Xiong, K. Zhu, X. Zhou, *RSC Adv.* **2015**, *5*, 31195–31204.
[174] Z. Kong, B. Yue, W. Deng, K. Zhu, M. Yan, Y. Peng, H. He, *Appl. Organomet. Chem.* **2014**, *28*, 239–243.

[175] S. Du, X. Chen, Q. Sun, N. Wang, M. Jia, V. Valtchev, J. Yu, *Chem. Commun.* **2016**, *52*, 3580–3583.
[176] J. Lin, F. Xin, L. Yang, Z. Zhuang, *Catal. Commun.* **2014**, *45*, 104–108.
[177] Y. Wang, M. Lin, A. Tuel, *Microporous Mesoporous Mater.* **2007**, *102*, 80–85.
[178] C. Pagis, A. R. Morgado Prates, D. Farrusseng, N. Bats, A. Tuel, *Chem. Mater.* **2016**, *28*, 5205–5223.
[179] T. Weissenberger, R. Leonhardt, B. A. Zubiri, M. Pitínová-Štekrová, T. L. Sheppard, B. Reiprich, J. Bauer, R. Dotzel, M. Kahnt, A. Schropp, et al., *Chem. – Eur. J.* **2019**, *25*, 14430–14440.
[180] V. Smeets, E. M. Gaigneaux, D. P. Debecker, *Microporous Mesoporous Mater.* **2020**, *293*, 109801.
[181] A. G. Machoke, A. M. Beltrán, A. Inayat, B. Winter, T. Weissenberger, N. Kruse, R. Güttel, E. Spiecker, W. Schwieger, *Adv. Mater.* **2015**, *27*, 1066–1070.
[182] L.-H. Chen, X.-Y. Li, G. Tian, Y. Li, J. C. Rooke, G.-S. Zhu, S.-L. Qiu, X.-Y. Yang, B.-L. Su, *Angew. Chem. Int. Ed.* **2011**, *50*, 11156–11161.
[183] W. Cheng, Y. Jiang, X. Xu, Y. Wang, K. Lin, P. P. Pescarmona, *J. Catal.* **2016**, *333*, 139–148.
[184] M. B. Yue, M. N. Sun, F. Xie, D. D. Ren, *Microporous Mesoporous Mater.* **2014**, *183*, 177–184.
[185] L. Lakiss, M. Rivallan, J.-M. Goupil, J. El Fallah, S. Mintova, *Catal. Today* **2011**, *168*, 112–117.
[186] C. Shang, Z. Wu, W. Duo Wu, X. Dong Chen, *Chem. Eng. Sci.* **2021**, *229*, 116080.
[187] D. P. Debecker, S. Le Bras, C. Boissière, A. Chaumonnot, C. Sanchez, *Chem. Soc. Rev.* **2018**, *47*, 4112–4155.
[188] C. Boissiere, D. Grosso, A. Chaumonnot, L. Nicole, C. Sanchez, *Adv. Mater.* **2011**, *23*, 599–623.
[189] M. Klumpp, L. Zeng, S. A. Al-Thabaiti, A. P. Weber, W. Schwieger, *Microporous Mesoporous Mater.* **2016**, *229*, 155–165.
[190] Z. Guo, G. Xiong, L. Liu, P. Li, L. Hao, Y. Cao, F. Tian, *J. Porous Mater.* **2016**, *23*, 407–413.
[191] V. Smeets, W. Baaziz, O. Ersen, E. M. Gaigneaux, C. Boissière, C. Sanchez, D. P. Debecker, *Chem. Sci.* **2020**, *11*, 954–961.
[192] A. Vivian, L. Fusaro, D. P. Debecker, C. Aprile, *ACS Sustain. Chem. Eng.* **2018**, *6*, 14095–14103.
[193] B. Karimi, H. M. Mirzaei, *RSC Adv.* **2013**, *3*, 20655–20661.
[194] A. Styskalik, I. Kordoghli, C. Poleunis, A. Delcorte, Z. Moravec, L. Simonikova, V. Kanicky, C. Aprile, L. Fusaro, D. P. Debecker, *J. Mater. Chem. A* **2020**, *8*, 23526–23542.
[195] X. Chen, P. Qian, T. Zhang, Z. Xu, C. Fang, X. Xu, W. Chen, P. Wu, Y. Shen, S. Li, et al., *Chem. Commun.* **2018**, *54*, 3936–3939.
[196] A. Vivian, L. Soumoy, L. Fusaro, S. Fiorilli, D. P. Debecker, C. Aprile, *Green Chem.* **2021**, *23*, 354–366.
[197] T. Blasco, M. A. Camblor, A. Corma, P. Esteve, A. Martínez, C. Prieto, S. Valencia, *Chem. Commun.* **1996**, 2367–2368.
[198] X. Fang, Q. Wang, A. Zheng, Y. Liu, Y. Wang, X. Deng, H. Wu, F. Deng, M. He, P. Wu, *Catal. Sci. Technol.* **2012**, *2*, 2433–2435.
[199] B. Wang, H. Han, B. Ge, J. Ma, J. Zhu, S. Chen, *New J. Chem.* **2019**, *43*, 10390–10397.
[200] D. T. Bregante, A. M. Johnson, A. Y. Patel, E. Z. Ayla, M. J. Cordon, B. C. Bukowski, J. Greeley, R. Gounder, D. W. Flaherty, *J. Am. Chem. Soc.* **2019**, *141*, 7302–7319.
[201] L. A. Rios, P. Weckes, H. Schuster, W. F. Hoelderich, *J. Catal.* **2005**, *232*, 19–26.
[202] Y. Awoke, Y. Chebude, C. Márquez-Álvarez, I. Díaz, *Catal. Today* **2020**, *345*, 190–200.
[203] A. Corma, M. T. Navarro, J. P. Pariente, *J. Chem. Soc. Chem. Commun.* **1994**, *0*, 147–148.
[204] P. T. Tanev, M. Chibwe, T. J. Pinnavaia, *Nature* **1994**, *368*, 321.
[205] C. J. Brinker, G. W. Scherer, *Sol-Gel Science: The Physics and Chemistry of Sol-Gel Processing*, Academic Press, **2013**.
[206] J. Livage, C. Sanchez, *J. Non-Cryst. Solids* **1992**, *145*, 11–19.
[207] D. P. Debecker, *Chem. Rec.* **2018**, *18*, 662–675.
[208] M. V. Landau, in *Handb. Heterog. Catal.*, American Cancer Society, **2008**, pp. 119–160.
[209] M. Dusi, T. Mallat, A. Baiker, *Catal. Rev.* **2000**, *42*, 213–278.
[210] R. Hutter, T. Mallat, A. Baiker, *J. Catal.* **1995**, *153*, 177–189.
[211] N. E. Thornburg, A. B. Thompson, J. M. Notestein, *ACS Catal.* **2015**, *5*, 5077–5088.
[212] Q. Du, Y. Guo, H. Duan, H. Li, Y. Chen, H. U. Rehman, H. Liu, *J. Alloys Compd.* **2017**, *699*, 386–391.
[213] O. Lorret, V. Lafond, P. H. Mutin, A. Vioux, *Chem. Mater.* **2006**, *18*, 4707–4709.
[214] Z. Wang, K. J. Balkus Jr., *Microporous Mesoporous Mater.* **2017**, *243*, 76–84.
[215] T. R. Eaton, A. M. Boston, A. B. Thompson, K. A. Gray, J. M. Notestein, *ChemCatChem* **2014**, *6*, 3215–3222.
[216] V. Lafond, P. H. Mutin, A. Vioux, *J. Mol. Catal. Chem.* **2002**, *182–183*, 81–88.
[217] H. Chu, C. Yu, Y. Wan, D. Zhao, *J. Mater. Chem.* **2009**, *19*, 8610–8618.
[218] R. Ch. Deka, V. A. Nasluzov, E. A. Ivanova Shor, A. M. Shor, G. N. Vayssilov, N. Rösch, *J. Phys. Chem. B* **2005**, *109*, 24304–24310.
[219] D. L. Evans, *J. Non-Cryst. Solids* **1982**, *52*, 115–128.
[220] M. Emili, L. Incoccia, S. Mobilio, G. Fagherazzi, M. Guglielmi, *J. Non-Cryst. Solids* **1985**, *74*, 129–146.
[221] R. De Clercq, M. Dusselier, C. Poleunis, D. P. Debecker, L. Giebeler, S. Oswald, E. Makshina, B. F. Sels, *ACS Catal.* **2018**, 8130–8139.

[222] L. Marchese, E. Gianotti, V. Dellarocca, T. Maschmeyer, F. Rey, S. Coluccia, J. M. Thomas, *Phys. Chem. Chem. Phys.* **1999**, *1*, 585–592.
[223] F. Babonneau, S. Doeuff, A. Leaustic, C. Sanchez, C. Cartier, M. Verdaguer, *Inorg. Chem.* **1988**, *27*, 3166–3172.
[224] Z. A. ALOthman, *Materials* **2012**, *5*, 2874–2902.
[225] C. Sanchez, J. Livage, M. Henry, F. Babonneau, *J. Non-Cryst. Solids* **1988**, *100*, 65–76.
[226] J. Livage, M. Henry, C. Sanchez, *Prog. Solid State Chem.* **1988**, *18*, 259–341.
[227] M. S. Rahman, J. Ambati, S. Joshi, S. E. Rankin, *Microporous Mesoporous Mater.* **2014**, *190*, 74–83.
[228] V. Smeets, C. Boissière, C. Sanchez, E. M. Gaigneaux, E. Peeters, B. F. Sels, M. Dusselier, D. P. Debecker, *Chem. Mater.* **2019**, *31*, 1610–1619.
[229] D. P. Debecker, P. H. Mutin, *Chem. Soc. Rev.* **2012**, *41*, 3624–3650.
[230] A. Styskalik, D. Skoda, C. E. Barnes, J. Pinkas, *Catalysts* **2017**, *7*, 168.
[231] A. Vioux, *Chem. Mater.* **1997**, *9*, 2292–2299.
[232] D. P. Debecker, V. Hulea, P. H. Mutin, *Appl. Catal. Gen.* **2013**, *451*, 192–206.
[233] V. Smeets, A. Styskalik, D. P. Debecker, *J. Sol-Gel Sci. Technol.* **2021**, *97*, 505–522.
[234] P. H. Mutin, A. Vioux, *Chem. Mater.* **2009**, *21*, 582–596.
[235] D. Skoda, A. Styskalik, Z. Moravec, P. Bezdicka, C. E. Barnes, J. Pinkas, *J. Sol-Gel Sci. Technol.* **2015**, *74*, 810–822.
[236] A. Styskalik, D. Skoda, J. Pinkas, S. Mathur, *J. Sol-Gel Sci. Technol.* **2012**, *63*, 463–472.
[237] Y. Jiang, Y. Zhao, X. Xu, K. Lin, D. Wang, *RSC Adv.* **2016**, *6*, 77481–77488.
[238] E. J. Zanto, S. A. Al-Muhtaseb, J. A. Ritter, *Ind. Eng. Chem. Res.* **2002**, *41*, 3151–3162.
[239] D. C. M. Dutoit, M. Schneider, A. Baiker, *J. Catal.* **1995**, *153*, 165–176.
[240] Y. Wan, Zhao, *Chem. Rev.* **2007**, *107*, 2821–2860.
[241] A. Taguchi, F. Schüth, *Microporous Mesoporous Mater.* **2005**, *77*, 1–45.
[242] J. Tang, J. Liu, J. Yang, Z. Feng, F. Fan, Q. Yang, *J. Colloid Interface Sci.* **2009**, *335*, 203–209.
[243] C. Anand, P. Srinivasu, G. P. Mane, S. N. Talapaneni, D. S. Dhawale, M. A. Wahab, S. V. Priya, S. Varghese, Y. Sugi, A. Vinu, *Microporous Mesoporous Mater.* **2012**, *160*, 159–166.
[244] C. G. Guizard, A. C. Julbe, A. Ayral, *J. Mater. Chem.* **1999**, *9*, 55–65.
[245] D.-S. Moon, J.-K. Lee, *Langmuir ACS J. Surf. Colloids* **2014**, *30*, 15574–15580.
[246] A. R. Oki, Q. Xu, B. Shpeizer, A. Clearfield, X. Qiu, S. Kirumakki, S. Tichy, *Catal. Commun.* **2007**, *8*, 950–956.
[247] M. C. Rogers, B. Adisa, D. A. Bruce, *Catal. Lett.* **2004**, *98*, 29–36.
[248] S. Flaig, J. Akbarzadeh, P. Dolcet, S. Gross, H. Peterlik, N. Hüsing, *Chem. – Eur. J.* **2014**, *20*, 17409–17419.
[249] A. Roucher, M. Depardieu, D. Pekin, M. Morvan, R. Backov, *Chem. Rec. N. Y. N* **2018**, *18*, 776–787.
[250] D. P. Debecker, C. Boissière, G. Laurent, S. Huet, P. Eliaers, C. Sanchez, R. Backov, *Chem. Commun.* **2015**, *51*, 14018–14021.
[251] V. Smeets, L. van den Biggelaar, T. Barakat, E. M. Gaigneaux, D. P. Debecker, *ChemCatChem* **2019**, *11*, 1593–1597.
[252] G. M. Pajonk, *Appl. Catal.* **1991**, *72*, 217–266.
[253] A. C. Pierre, G. M. Pajonk, *Chem. Rev.* **2002**, *102*, 4243–4266.
[254] M. Schneider, A. Baiker, *Catal. Rev.* **1995**, *37*, 515–556.
[255] H. Maleki, *Chem. Eng. J.* **2016**, *300*, 98–118.
[256] R. Mutter, D. C. M. Dutoit, T. Mallat, M. Schneider, A. Baiker, *J. Chem. Soc. Chem. Commun.* **1995**, *0*, 163–164.
[257] Y. Tao, P. P. Pescarmona, *Catalysts* **2018**, *8*, 212.
[258] C. A. Müller, R. Deck, T. Mallat, A. Baiker, *Top. Catal.* **2000**, *11*, 369–378.
[259] A. Sachse, V. Hulea, K. L. Kostov, N. Marcotte, M. Y. Boltoeva, E. Belamie, B. Alonso, *Chem. Commun.* **2012**, *48*, 10648–10650.
[260] S. Maksasithorn, P. Praserthdam, K. Suriye, M. Devillers, D. P. Debecker, *Appl. Catal. Gen.* **2014**, *488*, 200–207.
[261] V. Lafond, P. H. Mutin, A. Vioux, *Chem. Mater.* **2004**, *16*, 5380–5386.
[262] D. D. Dochain, A. Stýskalík, D. P. Debecker, *Catalysts* **2019**, *9*, 920.
[263] D. Skoda, A. Styskalik, Z. Moravec, P. Bezdicka, J. Bursik, P. Hubert Mutin, J. Pinkas, *RSC Adv.* **2016**, *6*, 68739–68747.
[264] A. Styskalik, V. Vykoukal, L. Fusaro, C. Aprile, D. P. Debecker, *Appl. Catal. B Environ.* **2020**, *271*, 118926.
[265] A. M. Cojocariu, P. H. Mutin, E. Dumitriu, F. Fajula, A. Vioux, V. Hulea, *Appl. Catal. B Environ.* **2010**, *97*, 407–413.
[266] V. Smeets, L. Ben Mustapha, J. Schnee, E. M. Gaigneaux, D. P. Debecker, *Mol. Catal.* **2018**, *452*, 123–128.
[267] C. Beck, T. Mallat, A. Baiker, *Catal. Lett.* **2003**, *88*, 203–209.
[268] T. Zhang, A. Solé-Daura, H. Fouilloux, J. M. Poblet, A. Proust, J. J. Carbó, G. Guillemot, *ChemCatChem* **2021**, *13*, 1220–1229.
[269] J. Silvestre-Alberó, M. E. Domine, J. L. Jordá, M. T. Navarro, F. Rey, F. Rodríguez-Reinoso, A. Corma, *Appl. Catal. Gen.* **2015**, *507*, 14–25.
[270] K. Lin, P. P. Pescarmona, K. Houthoofd, D. Liang, G. Van Tendeloo, P. A. Jacobs, *J. Catal.* **2009**, *263*, 75–82.

[271] M. B. D'Amore, S. Schwarz, *Chem. Commun.* **1999**, *0*, 121–122.
[272] L. E. Manangon-Perugachi, A. Vivian, P. Eloy, D. P. Debecker, C. Aprile, E. M. Gaigneaux, *Catal. Today* **2021**, *363*, 128–136.
[273] L. E. Manangon-Perugachi, V. Smeets, A. Vivian, I. Kainthla, P. Eloy, C. Aprile, D. P. Debecker, E. M. Gaigneaux, *Catalysts* **2021**, *11*, 196.
[274] M. Mazur, P. S. Wheatley, M. Navarro, W. J. Roth, M. Položij, A. Mayoral, P. Eliášová, P. Nachtigall, J. Čejka, R. E. Morris, *Nat. Chem.* **2016**, *8*, 58–62.
[275] M. Moliner, Y. Román-Leshkov, A. Corma, *Acc. Chem. Res.* **2019**, *52*, 2971–2980.
[276] M. K. Samantaray, E. Pump, A. Bendjeriou-Sedjerari, V. D'Elia, J. D. A. Pelletier, M. Guidotti, R. Psaro, J.-M. Basset, *Chem. Soc. Rev.* **2018**, *47*, 8403–8437.
[277] C. Hurt, M. Brandt, S. S. Priya, T. Bhatelia, J. Patel, P. Selvakannan, S. Bhargava, *Catal. Sci. Technol.* **2017**, *7*, 3421–3439.
[278] R. Gérardy, D. P. Debecker, J. Estager, P. Luis, J.-C. M. Monbaliu, *Chem. Rev.* **2020**, *120*, 7219–7347.
[279] O. A. Alimi, T. B. Ncongwane, R. Meijboom, *Chem. Eng. Res. Des.* **2020**, *159*, 395–409.
[280] M. L. Mohammed, R. Mbeleck, B. Saha, *Polym. Chem.* **2015**, *6*, 7308–7319.
[281] F. Liu, K. Huang, A. Zheng, F.-S. Xiao, S. Dai, *ACS Catal.* **2018**, *8*, 372–391.
[282] D. Cavuoto, F. Zaccheria, N. Ravasio, *Catalysts* **2020**, *10*, 1337.
[283] J. M. Fraile, J. I. García, J. A. Mayoral, *Chem. Rev.* **2009**, *109*, 360–417.
[284] S. Shylesh, M. Jia, W. R. Thiel, *Eur. J. Inorg. Chem.* **2010**, *2010*, 4395–4410.
[285] M. Bagherzadeh, M. Zare, M. Amini, T. Salemnoush, S. Akbayrak, S. Özkar, *J. Mol. Catal. Chem.* **2014**, *395*, 470–480.
[286] P. A. A. Ignacio-de Leon, C. A. Contreras, N. E. Thornburg, A. B. Thompson, J. M. Notestein, *Appl. Catal. Gen.* **2016**, *511*, 78–86.
[287] K. Zhang, O. K. Farha, J. T. Hupp, S. T. Nguyen, *ACS Catal.* **2015**, *5*, 4859–4866.
[288] D. P. Debecker, V. Smeets, M. Van der Verren, H. Meersseman Arango, M. Kinnaer, F. Devred, *Curr. Opin. Green Sustain. Chem.* **2021**, *28*, 100437.

Table of Contents

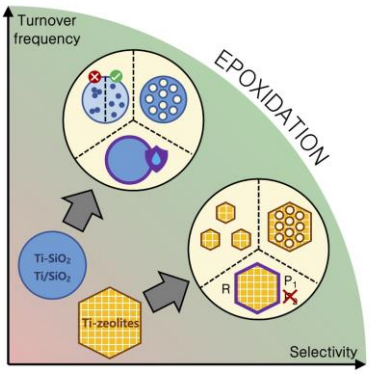

This review presents an overview of the recent advances in the development of titanosilicate catalysts used in epoxidation. Covering supported and grafted catalysts, microporous crystalline titanosilicates (including hierarchical zeolites), and amorphous titanosilicate obtained by sol-gel chemistry, we critically address the key relation between the preparation method and the physico-chemical properties that govern catalytic performance.